Graduate Theses, Dissertations, and Problem Reports

2002

Zinc pot bearing material wear rate as a function of contact pressure and velocity

James M. Snider II
West Virginia University

Follow this and additional works at: https://researchrepository.wvu.edu/etd

Zinc Pot Bearing Material Wear Rate as a Function of Contact Pressure and Velocity

By

James M. Snider II

THESIS

John Loth, Ph.D., Chair
Gary Morris, Ph.D.
Xingbo Liu, Ph.D.

Department of Mechanical and Aerospace Engineering

Morgantown, West Virginia
2002

Abstract

By
James M. Snider II

There are currently over 50 galvanizing lines in operation in the United States producing approximately 50 million tons per year of galvanized sheet. Frequently zinc-pot hardware fails which causes production delay, resulting in an economic loss. It takes approximately 3 hours to change the zinc-pot bearings at a downtime cost of $1600/h.

To predict the performance of the submerged bearings, a large number of variables must be considered. These variables include pot chemistry, temperature, line speed and line tension. With these variables it is possible to develop a design guide for sheet mill operators to determine the most cost-effective selection of zinc pot bearing materials/coatings, which will not be the same for all galvanizing lines.

The objective of this project is to measure wear rate of submerged zinc pot bearing materials as a function of contact pressure and velocity. A small laboratory size-testing machine was developed for this purpose. This machine measures the wear of bearing material samples, submerged in a cup of zinc, in the form a 1-inch diameter ball rotating against a matched ball seat. The seat and ball can be cast or machined using bearing materials from a test matrix. The seat is placed in a temperature controlled molten zinc bath where load, torque and RPM of the test samples are measured and recorded. From the measured torque the sliding friction coefficient of the bearing materials tested can be calculated. By measurement of the seat radius before and after testing, the wear rate of the material as a function of contact pressure and velocity was determined.

Acknowledgements

Contents

List of Tables

List of Figures

Nomenclature

A_B	Steel mill bearing area
A_{hor}	Horizontal projection of laboratory ball on seat contact area
$A_{hor,f}$	Final horizontal projected seat area
$A_{hor,i}$	Initial horizontal projected seat area
A_{seat}	Laboratory test sample seat contact surface area
F_B	Steel mill bearing contact force
F_{gage}	Force applied to the strain gage beam
F_{load}	Laboratory vertical spindle load by ball on seat
$F_{contact}$	Resultant of F_{Load} perpendicular to test sample contact surface
P_B	Steel mill bearing pressure
P_C	Laboratory ball on seat contact pressure
r_c	Mean contact radius of ball on seat
T_s	Sheet tension in galvanizing line
t	Time
TQ	Torque
V_B	Steel mill bearing contact surface velocity
V_C	Laboratory ball on seat contact velocity
V_{Sheet}	Velocity of sheet in galvanizing line
W_f	Final seat width
W_i	Initial seat width
ΔW	Change in seat width
μ_F	Friction coefficient
ω	Uncertainty function
ℓ_{gage}	Moment arm from spindle centerline to contact with strain gage beam

Chapter 1 - Introduction

This research project is a cooperative effort by West Virginia University, Industries of the Future of WV, International Zinc Research Organization, Oak Ridge National Laboratory, and various Steel Industries for the U.S. Department of Energy. All of these are working together to achieve a significant improvement in galvanizing line zinc-pot bearing life. The proposed five-year project consists of two phases. A multi-task approach is adopted for exploration and evaluation of new materials in Phase I for the first three years. The tasks for phase one include, computational design of new materials, corrosion tests of potential materials, coating technology assessment, wear and erosion tests of potential materials, and characterization and mechanistic study of the formation of interface layers and dross. Phase II consists of a scale up and pilot tests of new pot hardware. The life improvement of pot hardware is expected to be an order of magnitude over that of current standard materials used in molten metal baths.

The U.S. total steel production of 100 million tons/year has a value of approximately $40 billion. It has been estimated that 50% of the total steel production is sheet product, much of it sold in galvanized form. Frequent zinc-pot hardware failures increase the cost of energy to produce the product, which significantly reduces the profit margin. It takes approximately three hours to change the zinc-pot bearings at a downtime cost of $1600/h. Extending bearing life form one week to 3 weeks would save $163,000 a year. On a national scale, where there are 57 operational galvanizing lines, this would correspond to a yearly loss of approximately $27 million. Based on this, the need for new material technologies for pot hardware is critical and urgent for the U.S. steel industry.

Improvement of zinc-pot bearings would have a significant impact on the production cost of continuous hot-dip processes for value-added steel products.

Chapter 2 - Literature Review

2.1 New Material Research and Life Improvement for Pot Hardware

The coating of steel with protective metals such as zinc or aluminum is an economical means of providing corrosion resistance on various grades of steel. The coating of steel can be performed by a variety of processes, but continuous hot dipping process remains the most economical for mass production. The U.S. Department of Energy published the Steel Industry Road Map in March of 1998. This report indicated three main areas for steel product development consisting of containers, construction products, and automotive products. In each one of these product areas, coating technology was singled out as one of the high priority research and development needs. In order for steel to compete with other structural materials such as aluminum or fiber composites, hot dip operations require further reduction of manufacturing cost as well as energy consumption.

There are four main types of hot-dip coatings [1] developed as a standard in today's steel industry. All four coating materials are alloys of zinc and/or aluminum: 1. galvanize coating (Zn); 2. Galfan® coating (Zn-5%Al); 3. Galvalume® coating (45%Zn-Al); 4. Aluminize coating (Al-8%Si).

Current galvanizing lines operate continuously, but routine maintenance shutdowns are required periodically. One of the major factors that determine the frequency of shutdowns is the life of the roller bearings submerged in the molten zinc bath. The maintenance of roller bearings requires the cost of downtime in production, as well as the energy loss associated with restarting the continuous operation.

To ensure adequate performance operation, materials for pot hardware must be

carefully selected.   Failure to select the most suitable materials can lead to high maintenance costs, which may arise from extensive repair or replacement, premature and catastrophic failure, and decreased output because of downtime.   Satisfactory bath materials must posses the required mechanical strength at operating temperatures, be wear and corrosion resistant to the zinc composition inside the bath, be manufacturable into the desirable component shapes, and have a reasonable cost.

A variety of computer codes with extensive databases have been developed by others to enable researchers to predict the formation different phases on the surface of pot hardware materials.   ORNL and WVU have the experience to work with phase computation models in order to identify interface metallic compounds.

The IOF-WV steel group initiated a research team that included technical experts from West Virginia University and Oak Ridge National Laboratory in addition to engineers from West Virginia steel companies. A research team was set up to work on the most critical issues of new materials for pot hardware in continuous hot dip processes.

A typical arrangement for pot hardware is shown in Figure 1. As seen in this Figure, the components submerged in the molten zinc coatings are the rolls, bearings, and snout. The product quality of the hot-dip coating, especially uniformity of the coating layer, is strongly influenced by the condition of hardware submerged in the molten zinc bath.
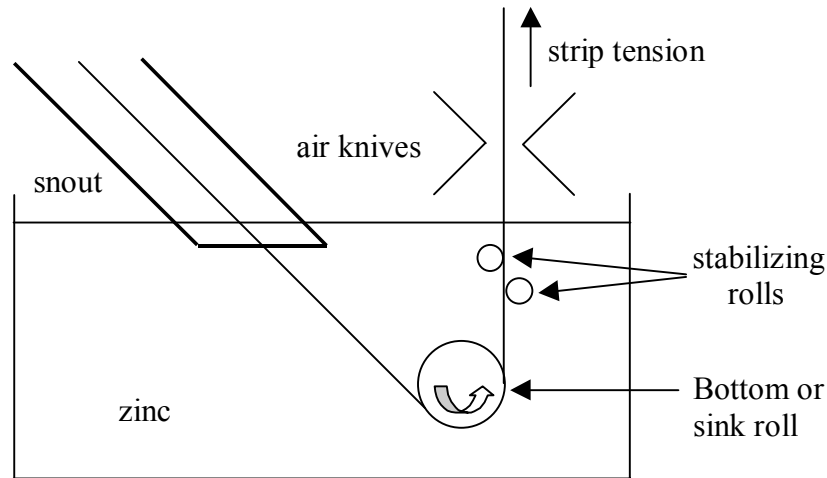
Figure 2.1: Diagram of Pot Hardware in Continuous Hot-Dip Process

There are two types of materials typically used in pot hardware. The rolls, including sink roll and stabilizing roll, are primarily made of 316L stainless steel. Roll bearings are generally made of cemented tungsten carbides, WC-Co, commercially known as Stellite #6. Both of these materials have been used in pot hardware for more than three decades. Their performance was found to be acceptable even before the hot-dip process became a fully automated and continuous operation. Based on an International Lead Zinc Research Organization (ILZRO) survey, the average life of pot hardware can vary from approximately seven days to six weeks, with approximately two weeks being the most common. The end of bearing life is dictated by the occurrence of one of the following in the production line: onset of roll skidding, onset of vibration, and no-concentric rotation.

2.2 BOCLE and HFRR Wear Testing

Based on available literature it is noted that dynamic wear testing of materials is done with materials being dry or lubricated. "The wear of lubricated bearing surfaces (Bond, et, al [2]) depends not only on the lubricant, but also on the materials used, the

bearing load, surface finish and velocity at the point of contact. Lack of sufficient lubricating properties increases wear, which alters the surface finish and produces loss of material from the surface. One can experience four types of wear: corrosion, adhesive wear, abrasive wear and surface fatigue. Wear can be reduced by the presence of lubricants and corrosion inhibitors at the point of contact of the wear bodies. Many testing machines have been built to perform these duties, like the four balls wear test, single particle wear test and the BOCLE test. Many have been developed to characterize lubricating fluids. The three most common test methods are: BOCLE (Ball-on-Cylinder Lubricity Evaluator), the HFRR (High Frequency Reciprocating Rig), and field-testing."

The BOCLE test (American Society for Testing and Materials, 1999 [3]) was designed for testing the lubricity of diesel and jet fuel. This test uses a 1/2 inch diameter ball placed on a cylinder rotating at 244 RPM submerged in the fluid being tested. The test is performed over a 30 minute period with a ball loaded to 9.81 Newtons force. After the test time has elapsed the scar on the ball is measured to the nearest 0.01 mm.

The Lubrizol Scuffing BOCLE test (Lubrizol Corporation, 2000 [4]) is a variation of the standard BOCLE test. This test applies a steady 7 kilogram load to the ball. The test is run for 2 minutes and then the scar on the ball is measured and used to determine the lubricating qualities of the test fluid.

The HFRR test (Rabinowicz, et, al [5]) uses a 1/2-inch ball that is rapidly vibrated back and forth over a flat surface. The ball is moved back and forth over a 1 mm stroke with a load of 200 grams. The time necessary to wear a scar into the ball is measured and the size of the scar is used to determine the lubricating qualities of the test fluid.

The BOCLE [2] "has been used for some time, but there are only a few of these machines available at specialty fuel testing labs. HFRR has been accepted by ISO, Society of Automotive Engineers (SAE) and is commonly used in Europe for testing diesel fuel lubricity. The drawback of HFRR is that, there are very few of these testing machines available in North America. Field-testing is good but very expensive."

2.3 Teck Cominco's Continuous Galvanizing Line Submerged Hardware Research

The Teck Cominco Product Technology Center in Canada has done extensive testing on characterizing the friction and wear of zinc pot bearing materials. Tests in molten zinc were conducted under simulated line operating conditions. The objective of Teck Cominco's study was to improve the life and performance of bearings submerged in molten zinc in galvanizing lines (Teck Cominco, 1996 [6]). In order to study the friction and wear characteristics of submerged bearing materials a pin on disk testing machine was designed and built, as seen in Figure 2.2. The machine was used to test various materials bearing materials used in zinc pot bearing hardware. It used an electric motor to drive a shaft that supports the testing materials. The materials were in the form of three pins that were installed in a hub that rotated on a fixed plate submerged in a molten zinc pot. The friction torque between the two materials was determined by measurement of the motor current. Contact load to the pins was provided by cylindrical weights on the drive shaft. The tests were performed over a zinc pot temperature range of $450^{\circ}C$ - $470^{\circ}C$. The bearing material wear was determined by measuring the loss of length of the pins and the depth of the wear groove on the disc.
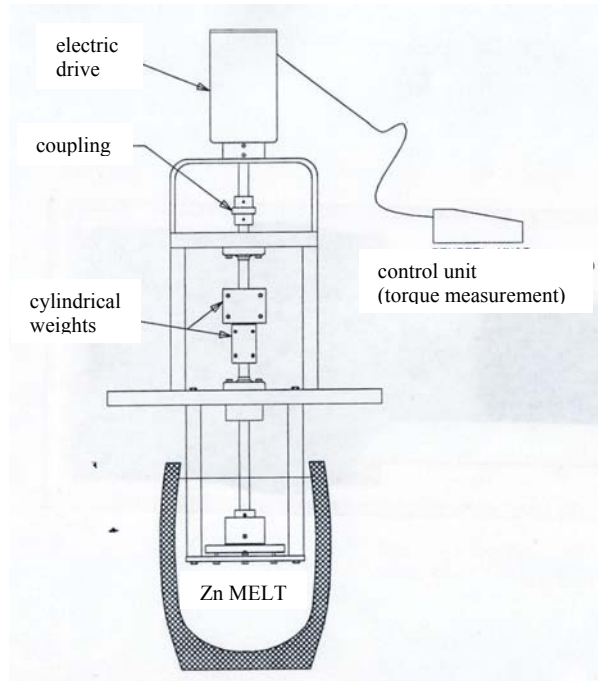
Figure 2.2: Diagram of Teck Cominco's Test Apparatus

Materials used in Teck Cominco's study include the following: 316 S.S., Inconel 718, Mild Steel with Alloy, 316 S.S., Stellite #6, Chromium Oxide coating, Tungsten Carbide coating, and Chromium Oxide lubricated. The testing showed that the friction coefficient of these materials ranged from 0.195 to 0.41. Figure 2.3 shows the results of Teck Cominco's friction coefficient testing [6]. The pin on disc wear of the material showed that wear was measurable [6], but in most cases insignificant, as seen in Table 2.1.
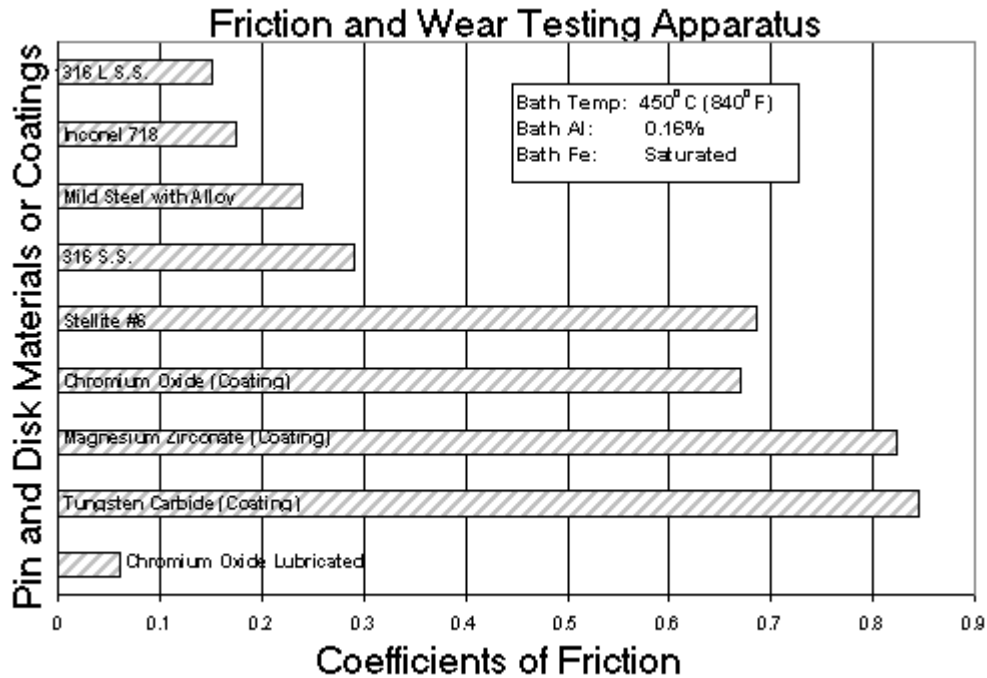
Figure 2.3: Teck Cominco's Friction Coefficient Data of Pin and Disc Materials

Table 2.1: Results from Teck Cominco's Wear and Friction Testing

Test Conditions: Bath Composition: 0.20 % Al, 0.0016% Fe
Melt Pot Temperature: 470°C

Plate Material	Pin Material	Coef. of Friction (μ)	Plate Wear (in)[mm]	Pin Wear (in)[mm]
Stellite #6	Stellite #6	0.29	--	0.0009 [0.023]
Stel. #6 with Graphite	Stellite #6	0.36	--	0.0005 [0.013]
Stel. #6 with Graphite*	Stellite #4	0.23	--	--
Tribaloy T-800	Stellite #4	0.39	--	0.0003 [0.008]
Triabaloy T-800	Stellite #4	0.37	--	0.0005 [0.013]
AmZirOx 86	AmZirOx 86	0.40	0.001 [0.025]	**
AmZirOx 86	Stellite #4	0.37	Light scoring	--
SIALON	Stellite #4	0.59	--	0.0004 [0.010]
SIALON***	Stellite #4	0.41	--	0.0005 [0.013]

   * Plate surface coated with graphite lubricant spray prior to test.
   ** Pin wear not measured, pins fractured on removal from test rig.
   *** Sialon plate polished to ensure flat surface.

      In order to evaluate the attack by the molten zinc alloy, a static immersion test

was used [7]. The samples were weighed before and after into the zinc pot to determine

loss per unit area. As seen in Table 2.2 the loss per unit area ranged from 0.7 g/dm^3 to 32.8 g/dm^3.

Table 2.2: Teck Cominco's Static Immersion Tests

Test Conditions: Zinc alloy: Zn + 0.2% Al + 0.022% Fe
Temperature: 470°C
Time: 96 Hours

Material	Loss / Unit Area (g/dm^2)
AmZirOx86	*
SIALON	*
Tribaloy T-800	0.7
Stellite #6	1.9
Inconel 718	2.5
316L S.S.	2.8
Mild Steel	32.8

The main conclusion drawn from Teck Cominco's submerged zinc pot hardware research was that metallic materials reacted with the bath to form intermetallics. The formation of intermetallics was shown to be dependent on zinc composition and zinc pot temperature. The formation of intermetallics also affects the friction and wear of the material. Teck Cominco found that aluminum in the zinc composition had a strong effect on friction and wear, while lead and antimony had no effect.

Next, Teck Cominco designed and built a testing machine to simulate actual steel mill galvanizing line conditions. The Teck Cominco full journal-bearing tester is capable of testing full size stabilizer rollers of half size sink roll bearings. In the machine design a motor and shaft supports a hollow drive shaft inclined at 30 degrees from horizontal. The test specimen is secured to the end of the drive shaft with a tapered fit. A tension compression load cell is used to measure the bearing load provided by a hydraulic system. A heated zinc pot sits below the test bearing and is raised into position by a hydraulic stacker.

The wear tests were performed under typical galvanizing line operating conditions. "The bushings used for testing the liquid zinc were modified by giving them larger clearance on their unloaded side so that experimental work was facilitated. Four tests were run with the low-load air cylinder to examine hydrodynamic operation and one test with the hydraulic cylinder, fully testing the capabilities of the apparatus. Significant zinc attack was seen on all materials after testing. In one case dross was encouraged to enter the bearing clearance by allowing the bath level to drop to the clearance height allowing dross entry. This was found to give particularly severe wear. In general this apparatus appears to be well suited for simulation of pot hardware bearing operations as they happen on sheet galvanizing lines." The results of the zinc attack on both 316L stainless steel and Stellite #6 can be seen in Tables 2.3 and 2.4 respectively.

Table 2.3: Results of EDS Analysis on the Alloy Layers of the 316L Bushing

Probe Location	Elements Analyzed (Normalized wt%)						
	Zn	Fe	Al	Cr	Ni	Mo	Si
Surface crystal particle (A)	92.4	5.2	1.8	0.3	0.4	---	---
Upper amorphous layer (B)	87.2	6	3.6	0.6	0.6	1.4	0.5
Lower amorphous layer (C)	73.8	13.4	9.1	1	0.9	1.2	0.6
Interface line (D)	59.8	20.4	15	1.5	1.3	1.3	0.8
Stainless steel substrate	---	71.5	---	14.7	12.2	1.3	0.4

Table 2.4: Results of EDS Analysis on the Alloy Layers of the Stellite #6 Sleeve

Probe Location	Elements Analyzed (Normalized wt%)						
	Zn	Co	Fe	Cr	W	Al	Mo
Surface crystal particle (A)	94.5	3.1	2.1	0.4	---	---	---
Alloy layer (B)	79.2	8.9	2.9	2.2	4.4	2.5	---
Stellite dendrite structure	---	76.6	2.6	19.6	0.8	---	0.4
Stellite inter-dendritic structure	---	18.2	1	79.3	1	---	0.5

2.4 WVU's Lubricity Research and Testing Apparatus

In 1998, during a methanol fueled gas turbine test at West Virginia University, the fuel controller bearings seized. This indicated the need for an additive to improve methanol lubricity properties. Many fuel additives for the methanol auto racing industry were available on the market. In order to minimize operational costs associated with adding fuel lubricant, a new friction test apparatus was designed to measure the friction coefficient of the bearing materials used in the GTC-85 gas-turbine fuel controller with various additives. Fuel additive cost was based on required concentration multiplied by cost per gallon. The minimum concentration required was defined so as to equalize bearing friction inside methanol to that of kerosene or Jet-A aviation grade kerosene. A new apparatus was designed, in order to eliminate the vibrations and erratic data produced by the existing WVU wear testing apparatus. The objective of that research was to find the most cost effective fuel additive for methanol capable of providing lubricity equal or better than that of jet fuel.

The new testing apparatus at WVU was designed to operate at typical gas-turbine bearing pressures by using a dead weight attached to the spindle, as seen in Figure 2.4. The spindle transferred the load to a disk containing three balls, which rotated on a fixed plate. A ball bearing was installed on the centering pin in the center of the fixed plate to insure that the disk rotates smoothly about its axis. To maintain constant RPM during the test, a vertical mill with variable speeds was used as a driver.
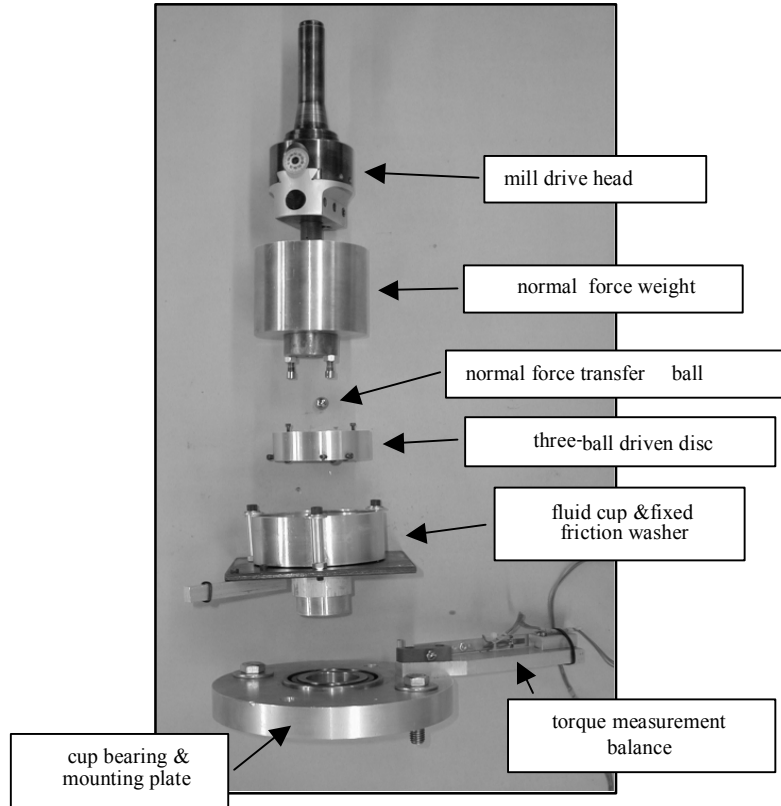
Figure 2.4: WVU Lubricity Test Apparatus

Torque is transferred from the drive shaft to the 6 lb$_f$ dead weight by use of a horizontal shear pin. From that pin via two vertical pins to the rotating 0.5 inch ball holder. A cup filled with methanol and fuel additive contains a ground washer on which the three balls rotate. The three balls had flat contact surfaces ground on them to reproduce recommended contact pressures for bronze bearings. The torque was measured with a beam type load cell.

Each run of the test apparatus was for 10 minutes at 3.5% of a lubricated bearing design load and provided repeatable data. Compared to the previously available WVU test equipment, this apparatus showed significant improvement. Table 2.5 shows typical

friction coefficients for various materials from the Machinery's Handbook [8]. Table 2.6

shows the fuel calibration test results for methanol fuel and for Jet A, the standard gas

turbine fuel.

Table 2.5: Machinists Handbook Friction Coefficients

System	Friction Coefficient
Metal on Metal (Dry)	0.15-0.20
Metal on Metal (Wet)	0.3
Occasionally Greased	0.07-0.08
Continuously Greased	0.05
Mild Steel on Brass	0.44

Table 2.6: Results of WVU's Friction Coefficient Test Apparatus

System	Friction Coefficient
LPMEOH^{TM} Methanol (Mild Steel on Brass)	0.309
Jet A (Mild Steel on Brass)	0.167

Based on the effects of fuel additives on friction coefficient, shown in Figure 2.5,

it was decided to continue operation of the gas turbine on methanol, but with 0.2% of a

commercial fuel additive.
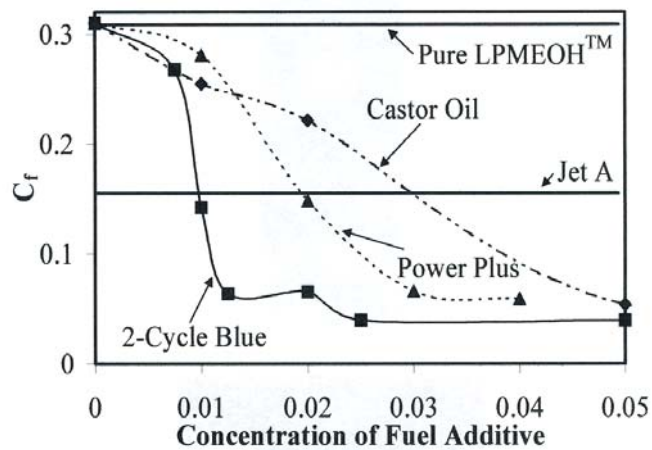
Figure 2.5: Effect of Fuel Additives on Friction Coefficient

2.5 Zinc Pot Bearing Material Research

The primary reason for galvanizing line stoppage is zinc pot bearing wear and associated line vibrations, which effects the appearance of the galvanized sheet, or create problems with steering the sheet. A case study performed by (Zoz, et, al [9]) shows the advantage of replacing common bearing materials with advanced materials and coatings. Stellite #6 is a common bearing material that has poor physical lubricating properties but, is corrosion resistant and does not contribute to dros build-up. Zoz used various materials for testing made of Stellite-4 powder with two different alloying elements, A+B, under each of 3 different parameter settings, 1-3, shown in Figure 2.6. A process control agent had to be added for the use of alloying element B. The test required test samples were made by Hot Isostatic Pressing (HIP) (El-Madg et, al [10]) using powder consolidation. Ten new material Stellite samples were consolidated into test specimens. To evaluate the wear behavior of these samples, Zoz, et, al [9] designed a cylinder and bush test apparatus (CIBA).
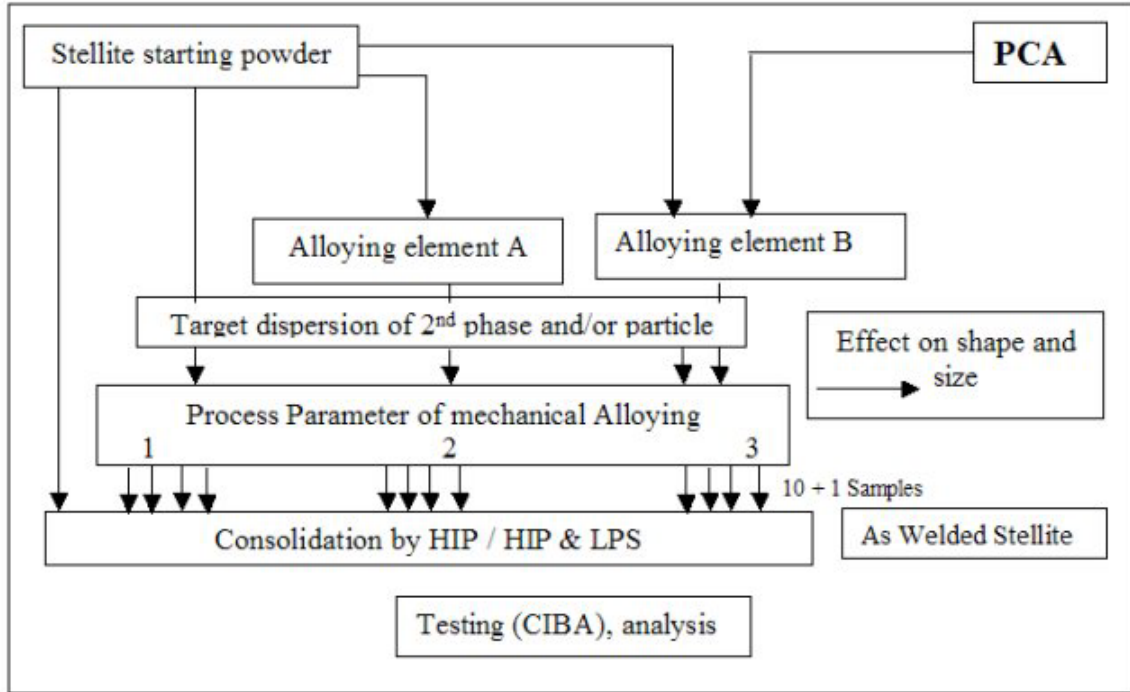
Figure 2.6: Flow Chart of Powder Production by Hot Isolated Pressing [9]

Zoz, et, al describes the CIBA as follows: "The inner part of the bearing system (bush fixed on the rolls) is simulated by the bulk sample itself (cylinder), carrying the new materials as well as the reference material. The outer part of the bearing (bush) is simulated by real Stellite counter-bearing parts." The bush is lowered into a zinc bath, then loaded and rotated against the cylinder, by a drilling machine, to simulate wear in hot dip galvanizing line processes.

The CIBA experiments have shown better wear resistibility in the bearing test samples than in operating galvanizing lines. Also, any dependency between hardness and abrasion resistance was not observed. The test samples did not show any cracks, inclusions, hollows, or binding failures in the diffusion zone between inner cylinder and consolidated material.

There are many types of commercially available composite coatings; the most popular of which is tungsten carbide (WC). These materials can be laser cladded on a variety of base materials including stainless steel and ORNL 4. In Surface and Coatings Technology Journal are articles describing the effects of tungsten carbide laser coatings submerged in zinc. Laser surface cladding (Seong, et, al [11]) is capable of producing a wide range of surface alloys and composites based on desired properties. "Application of the laser beam cladding surface engineering [11] allows to obtain porosity and crack free surface clads containing uniformly distributed hard particles in the softer and tough matrix." The structure of tungsten carbide laser cladding depends on the correct selection of the laser processing parameters to achieve porosity and crack free WC-metal composite coatings.

Studies have been done that look at the effects of molten zinc reacting with the tungsten carbide coating. Understanding the coating degradation processes [11] is very important for the development of better coatings for CGL pot rolls. WC–Co coating usually does not exceed 100 days. Dross build up on the zinc rollers degrades coating quality.

Experiments have been conducted (Seong, et, al [11]) in which rollers have been immersed in molten zinc to examine the effects of zinc attack on the coating. Dozens of dross specimens were collected for comparisons of reaction products and were analyzed with a scanning electron microscope and energy disperse spectrum. The experiments determined that aluminum in molten zinc reacted with the coating layer along cracks and diffused into the coating with similar diffusion depths.

Various companies have measured the friction coefficient and wear of submerged zinc pot roller bearings in molten zinc. This was in an effort to help design better test rigs and apparatus. Tests have proven that the temperature of the molten zinc has a strong effect on bearing materials and coatings. The zinc composition used can break down the structure of the bearing material and coating. It was discovered that materials with the best wearing properties may not have the lowest friction coefficient.

Research has been done to determine the effects of the molten zinc on the bearing materials. Static immersion tests were done to show how materials and coatings react with zinc. New zinc bath compositions have been researched for the best reaction with the bearing materials and coatings. Bearing materials like Stellite #6 and tungsten carbide coatings have been found to provide long lasting bottom roller bearing materials.

2.6 Arcelor Research's Bearing Tester for Bath Hardware Material

Arcelor Research developed an apparatus to measure friction coefficient and wear of zinc pot bearing materials. "Friction and wear [12] of sleeves and bushings is a main concern for Galvanizers, and cause: poor rotation quality, poor product quality, lowering of line speed, unexpected line stops, and high cost maintenance stops." The objective of the study at Arcelor is to determine the influence of sleeves/bushing friction phenomenon exactly as in an industrial zinc pot and to obtain results that are usable by industrial galvanizing lines.

The apparatus designed for testing zinc pot bearing materials used the same applied force and rotation speed as in industrial lines. The tester was capable of applied forces up to 50,000 N and rotation speeds up to 160 m/min. A 1000 kg controlled

temperature zinc pot with chemical analysis was used, as seen in Figure 2.7. The apparatus used a 150-mm sleeve, shown in Figure 2.8, to simulate the zinc pot bottom bearing rollers.

Figure 2.7: Picture of Arcelor's Test Apparatus

Figure 2.8: Picture of Arcelor's Test Specimen

Arcelor's test apparatus has the ability to measure applied force, rotation speed, and bath and bearing temperatures. This machine can also measure friction torque and wear by use of a position sensor. Tests were run for 4 days at an equivalent line speed of 120 m/min and 24,000 N force for Stellite #6 on Stellite #6. Friction torque and wear data were collected and used to calculate friction coefficient. The friction coefficient and wear as a function of time can be seen in Figures 2.9 and 2.10 respectively.
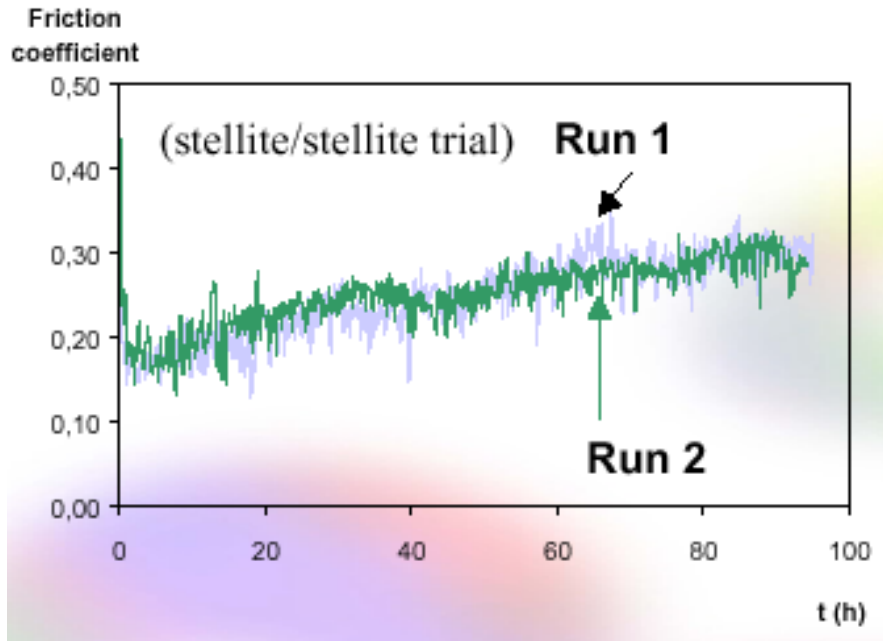
**Figure 2.9: Friction Coefficient as a Function of Time for
Stellite #6 on Stellite #6 in Arcelor's Tester [12]**
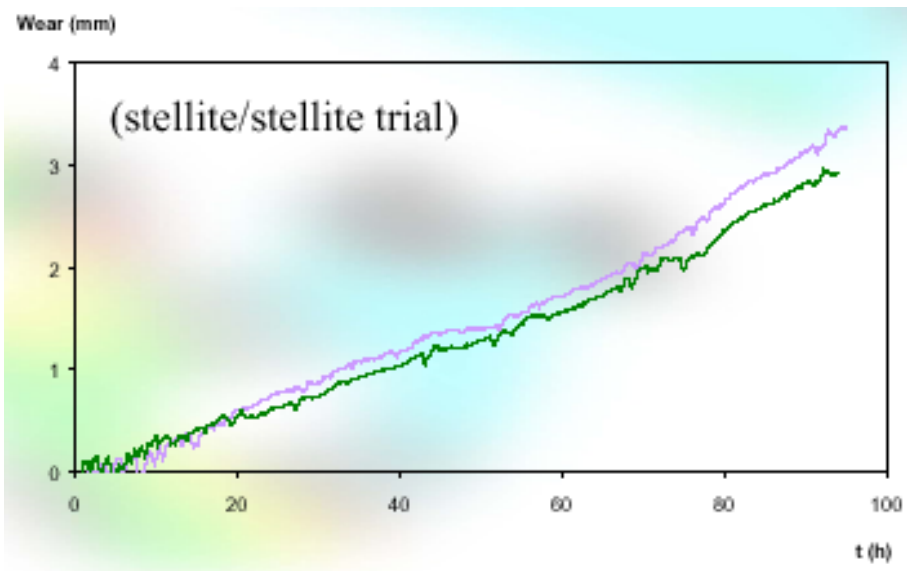
**Figure 2.10: Wear as a Function of Time for
Stellite #6 on Stellite #6 in Arcelor's Tester [12]**

Arcelor's test run indicates that the wear of Stellite #6 on Stellite #6 is linear with time. Figure 2.11 shows that at different bearing loads the wear as a function of time remains linear. The friction coefficient calculations indicated that the coefficient became

constant only after long periods of time. A friction coefficient of 0.14 was determined

after 3 hours of testing, but a friction coefficient of 0.30 was determined after 4 days of

testing as seen in Figure 2.12. This may be caused by the time required to properly "seat"

the bearing surfaces.
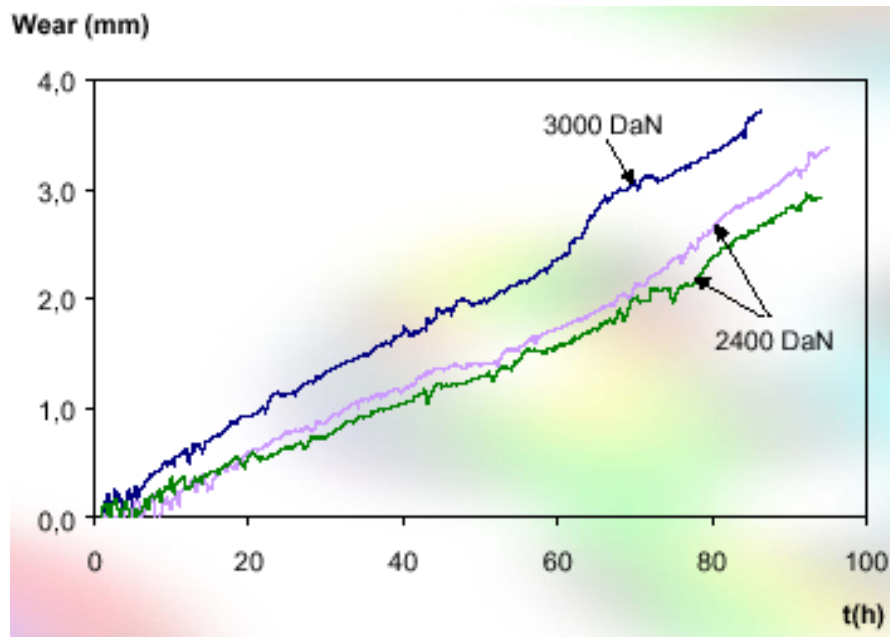
**Figure 2.11: Wear as a Function of Time at Different
Applied bearing Loads for Stellite #6 on Stellite #6 [12]**
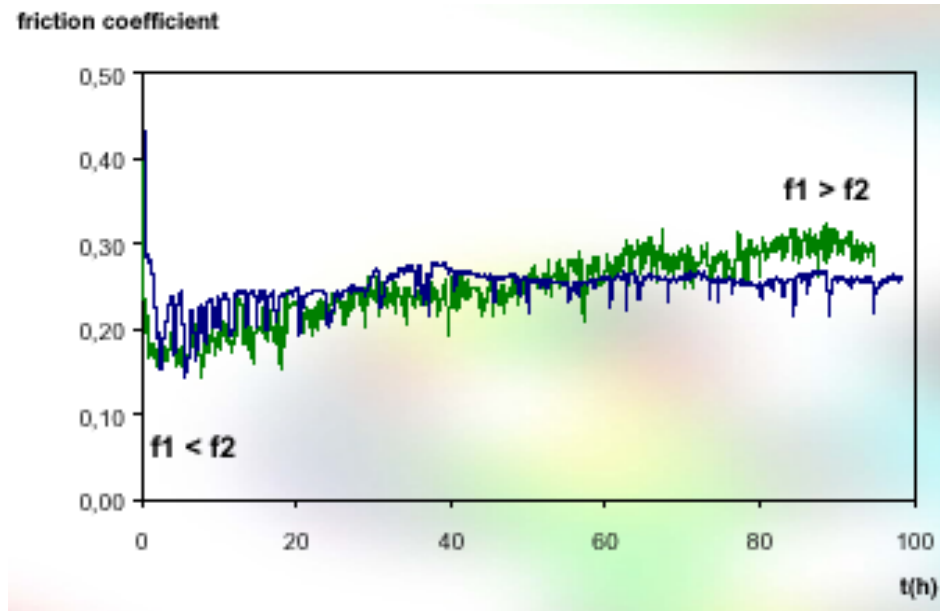
**Figure 2.12: Evolution of Friction Coefficient with
Time for Stellite #6 on Stellite #6 [12]**

2.7 WVU's Zinc Pot Bearing Materials Tester

A new machine designed specifically for testing zinc pot bearing materials was developed at West Virginia University by Dr. John Loth and Ryan Ware [13]. The design objectives were:

a) Provide repeatable friction coefficient and material wear data for bearing material comparison.

b) Minimize cost to prepare, install, and analyze test samples.

c) Test sample geometry selected was a 1-inch ball surface mounted on a spindle, which rotates on a stationary sample, with a narrow seat machined into it, at a 45° contact angle.

d) Automate data acquisition by using high sampling rate.

e) Provide pneumatic cushioning of the stationary sample so as to eliminate vibration and load changes and simplifying load adjustment.

f) Use small stainless steel cups, within each is mounted a stationary sample. The cup is then filled with zinc taken from an actual zinc pot.

g) Use an inexpensive vertical mill to drive a water-cooled spindle containing the 1-inch hemisphere test sample.

This apparatus was designed to simulate actual steel mill galvanizing line machine bearing operating conditions, as shown in Figure 2.13 and Table 2.7. These typical steel mill galvanizing line operating conditions were provided by Weirton Steel.
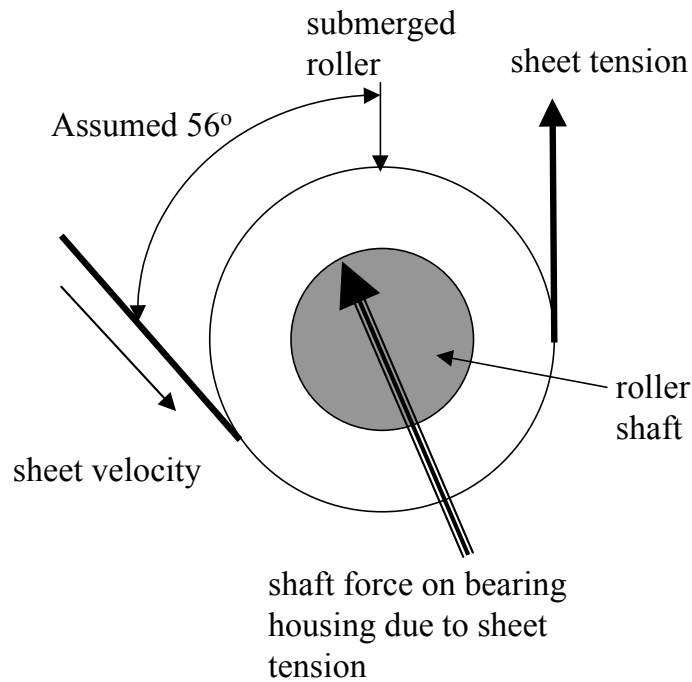
Figure 2.13: Schematic of Galvanizing Line Roller and Bearing

Table 2.7: Weirton Steel Operational Galvanizing Lines Data Ranges

	Line #3	Line #4	Line #5
Pot liner	Ceramic Brick	Ceramic Brick	Ceramic Brick
Zinc pot chemistry	0.08-0.22% Al	0.15-0.22% Al	0.08-0.22% Al
Temperature	880 - 1100°F	900 - 940°F	880 - 900°F
Sheet width	24 - 49 inch	24 - 42 inch	24 - 49 inch
Sheet thickness	.028 - .165 inch	.0094 - .028 inch	.012 - .045 inch
Sheet tension (T_s)	3200 - 5000 lbf	1000 - 2000 lbf	3200 - 4800 lbf
Sheet velocity	50 - 300 ft/min	100 - 410 ft/min	110 - 550 ft/min
Bottom Roller Characteristics			
Bearing life	7 - 14 days	7 - 14 days	7 - 30 days
Bearing materials	316L S.S.	316L S.S.	316L S.S
Outside diameter (D_R)	24 inch	20 inch	20 inch
Shaft diameter (D_B)	5.25 inch	3.875 inch	3.875 inch
Bearing length	4 inch	4 inch	4 inch, three 1-inch inserts
Each bearing has projected area (A_B)	21 inch^2	15.5 inch^2	9.65 inch^2

To correlate Weirton Steel operational data to the WVU zinc pot bearing material tester, an average sheet entry angle of 56° from vertical was assumed. From the configuration shown in Figure 2.13, each of the two bearings at the end of the roller carries a load F$_B$ related to the sheet tension, F$_{sheet}$, by:

$$F_B = T_S * [(\cos(0.5 * 45°)] = 0.88 * T_S \qquad \textbf{(2.1)}$$

The bearing contact pressure was determined by a ratio of bearing force, F$_B$, over the contact area of one of the two bearings.

$$P_B(psi) = \frac{F_B}{A_B} = 0.88 * \left(\frac{T_S}{A_B} \right) \qquad \text{(2.2)}$$

The bearing contact velocity is lower than the sheet velocity, which equals the roller surface velocity.

$$V_B = V_{Sheet} * \left[\frac{D_B}{D_{Roller}} \right] \qquad \text{(2.3)}$$

With the use of equations 2.1 through 2.3 steel mill bearing pressures and velocities were determined. Table 2.8 shows the velocity of the bearing and the bearing pressure in the zinc pot galvanizing lines.

Table 2.8: Correlation Between Steel Mill and Tester Operating Conditions

	Line #3	Line #4	Line #5
Projected Contact Area of Each Bearing, A_B (inch^2)	21	15.5	9.65
Line Speed (ft/min)	50 - 300	100 – 410	110 – 550
Line Tension, T_S (lb$_f$)	3200 - 5000	1000- 2000	3200 – 4800
Bearing contact V_B (inch/s)	2.19 – 13.1	3.88 – 15.9	4.26 – 21.3
Bearing contact P_B(psi)	134 – 210	57 – 114	293 – 440

West Virginia Universities' zinc pot bearing materials tester uses a 1 inch ball rotating on a stationary seat, machined as shown in Figure 2.14. This design is based on a 45° average contact angle or mean contact diameter of 0.707 inches. The 5/8-inch hole in the seat results in an outer diameter of 0.780-inches. This is fabricated by sinking a 1-inch ball mill to the depth of 0.187-inches. The resulting horizontal projected area A_{hor} = 0.171 square inches.
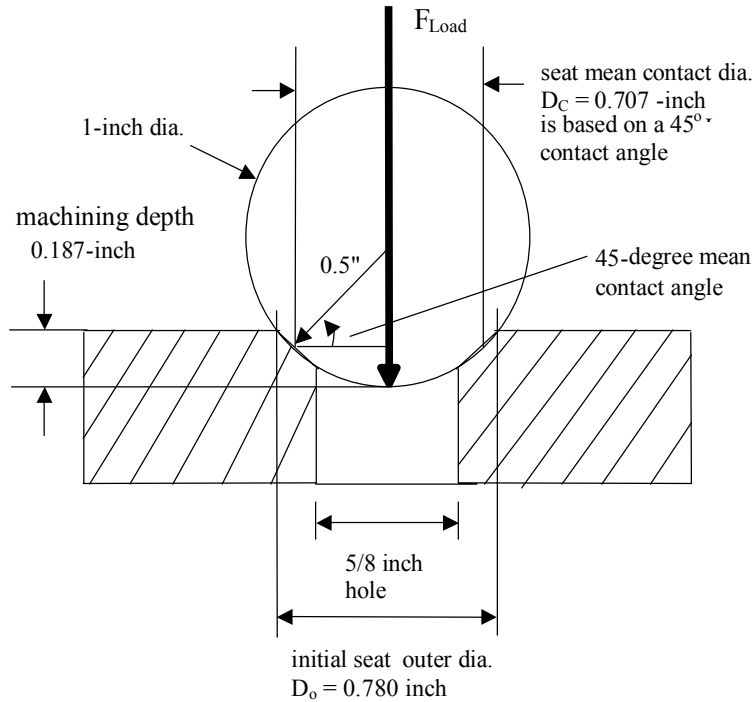
Figure 2.14: Ball and Seat Specimen Diagram

In order to duplicate steel mill operating bearing pressures, P_B (psi), in the bearing materials tester the ball specimen containing spindle was loaded to F_{Load} to produce the desired bearing contact pressure, P_c.

$$P_B = P_C = \frac{F_{Load}}{A_{Hor} = 0.171} = \frac{F_{\perp}}{A_{Seat}} \qquad \text{(2.4)}$$

Based on the 0.780-inch seat outer diameter, the contact velocity for the sample specimens was determined.

$$Ball\ RPM = V_C(inch/s)*[60/(0.707*\pi) = 27] = V_C(ft/s)*324 \quad \text{(2.5)}$$

With the use of the above equations the operational data ranges provided by Weirton Steel were converted to equivalent operational ranges for WVU's bearing materials tester, as shown in Table 2.9.

Table 2.9: Weirton Steel Operational Ranges Converted to WVU's Zinc Pot Bearing Materials Tester (* operating conditions are common to both)

	Line #3	Line #4	Line #5
Line Speed (ft/min)	50 – 300	100 – 410	110 – 550
Line Tension (lb)	3200 - 5000	1000- 2000	3200 – 4800
*Bearing contact V_C (inch/s)	2.19 – 13.1	3.88 – 15.9	4.26 – 21.3
*Bearing contact P_B (psi)	134 – 210	56.8 – 114	292 – 438
Tester Ball RPM	59.3 – 365	34.3 – 429	117 – 575
Tester Ball Load (lb)	23 – 36	9.71 – 19.4	50 – 74.9

A vertical mill/drilling machine was used to drive WVU's zinc pot bearing materials tester. This machine provides the constant RPM and load needed. A 2500-Watt melting pot was used to melt and maintain tin to the desired temperature. The outside dimensions of the zinc pot are 10-inch diameter by 10-inch tall, with inside dimensions 6-inch diameter by 6-inch height. The 1/4-inch aluminum disc covering the pot is suspended on a 1/4-inch diameter ball bearing track. This disc supports the cup holder. The friction torque transmitted from the spindle to the ball seat inside the zinc containing cup is transferred via the cup holder to the disc. A bracket attached to this disc transfers this torque to a strain gage beam, connected to the data logger. The water-cooled aluminum ring with the 1/4-inch ball bearing track is attached to three 3/4-inch linear bearings, which allow it to move up and down friction free. The ring rests on a PVC plate floating on an inner tube, as shown in Figure 2.15. The tube in turn rests on another plate supported by three load measuring strain gage balances. Two of these are used for a digital load indicator, while the third gage is used for computer data logging. Figure 2.16 shows a picture of the bearing track assembly and cup torque transfer plate.
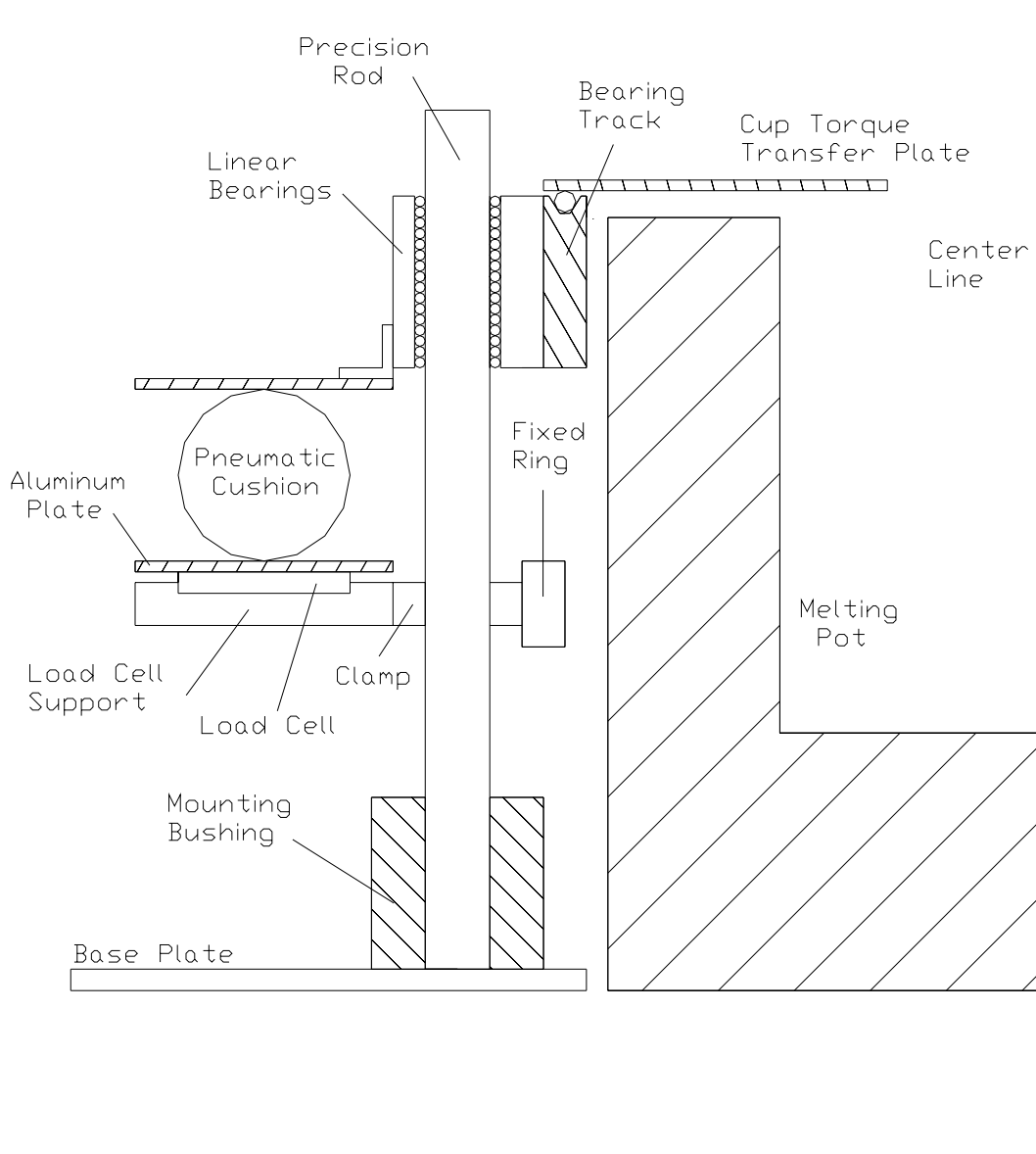
Figure 2.15: Cross Section of the Bearing Track Assembly
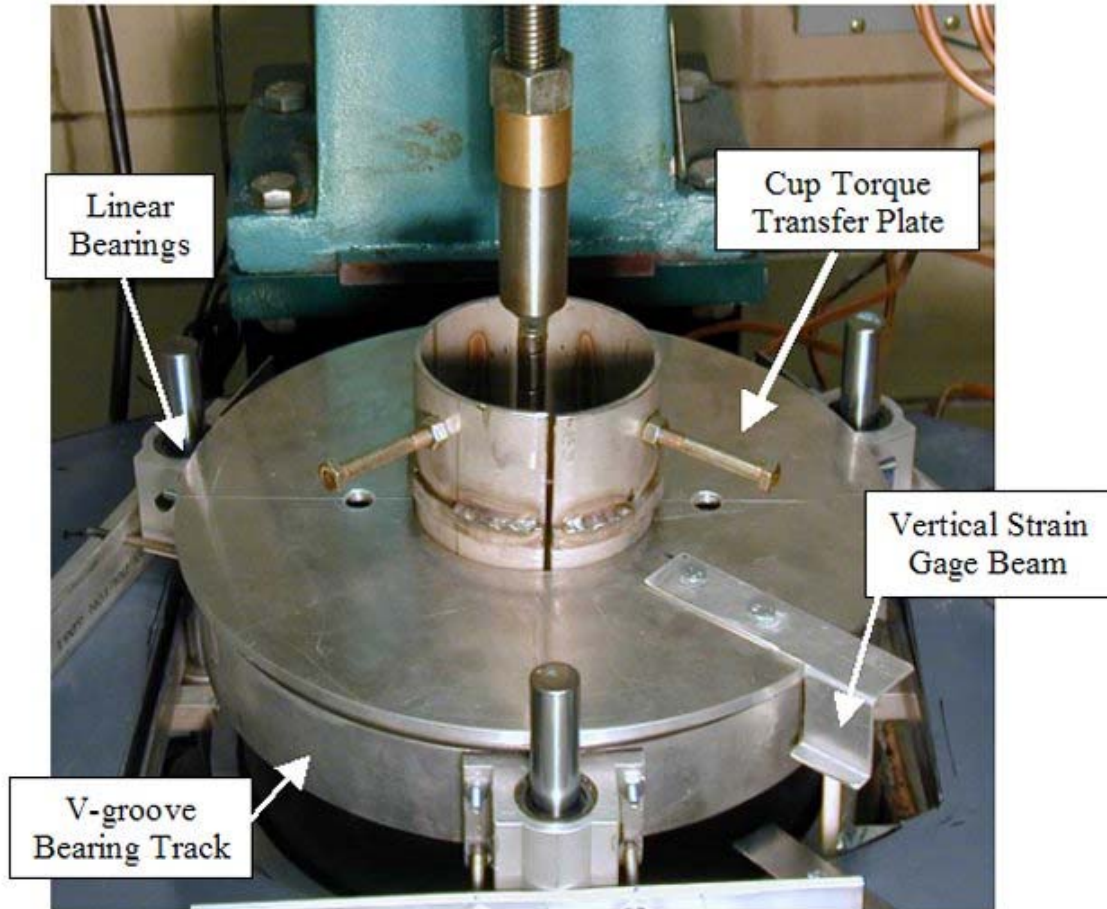
Figure 2.16: Picture of Bearing Track Assembly and Cup Torque Transfer Plate

The ball specimen was held in place by the use of a spindle. The bearing track assembly and mill bed were both cooled by use of water lines. Using the large contact area of a 5-inch aluminum disc to transfer the heat to a stationary water-cooled mating disc cooled the spindle. They made contact under spring pressure, see Figure 2.17.
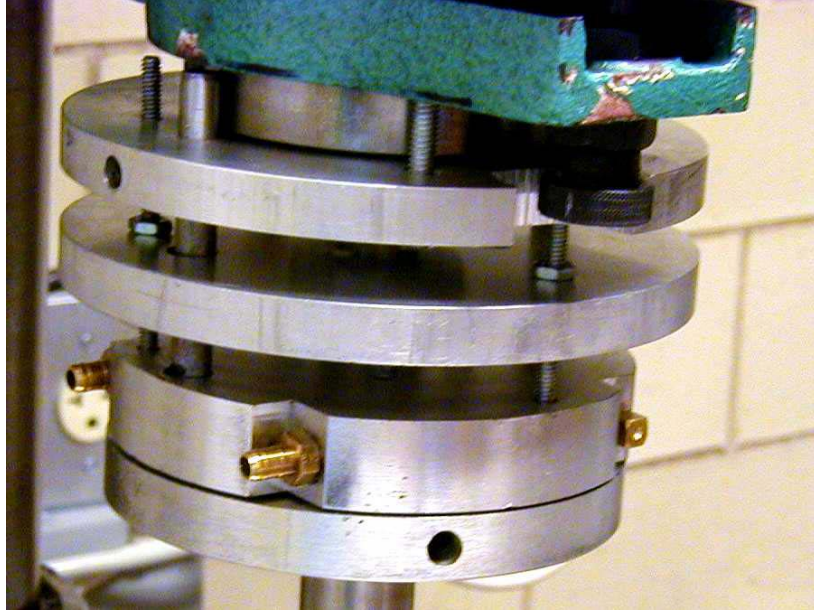
Figure 2.17: Water Cooled Spindle

The WVU wear tester is capable of testing a variety of zinc pot bearing materials. These materials include Stellite 6, MSA 2012, ORNL 4 (with WC-Laser Cladding), and 316 Stainless Steel (with WC-Laser Cladding). Stellite 6 and Stainless Steel are the most widely used bearing materials. Before testing, all materials were polished using three grades of diamond-lapping compound. An initial test matrix of the materials to be tested can be found in Table 2.10.

Table 2.10: Initial Material Test Matrix

	Seat: 316SS	Seat: 316SS with Laser Cladding	Seat: Stellite #6	Seat: ORNL-4 with Laser Cladding	Seat: MSA 2012
Ball: 316 SS	Trial Test	Trial Test	Trial Test	Trial Test	Trial Test
Ball: Tungsten	Trial Test	Trial Test	Trial Test	Trial Test	Trial Test
Ball: 316SS with Laser Cladding			Test		Test
Ball: Stellite #6		Test	Test	Test	Test
Ball: ORNL-4 with Laser Cladding			Test		Test
Ball: MSA 2012		Test	Test	Test	Test

Most materials in the test matrix can be machined, but some must be cast. One of the materials that must be cast is the ORNL 4 ball and seat specimens. This was done by the use of a cope and drag sand mold, design and constructed at WVU.

The seat specimen was held in place by the use of a stainless steel strut channel. This channel was then bolted to the inside of the specimen test cup. The stainless steel strut channel and specimen test cup with attached channel can be seen in Figures 2.18 and 2.19 respectively.

Figure 2.18: Stainless Steel Strut Channel and Seat

Figure 2.19: Stainless Steel Strut Channel and Seat Bolted into Specimen Cup

Figure 2.20 shows the assembled WVU zinc pot bearing materials tester. This machine was used to test the friction coefficient and wear of zinc pot bearing materials.
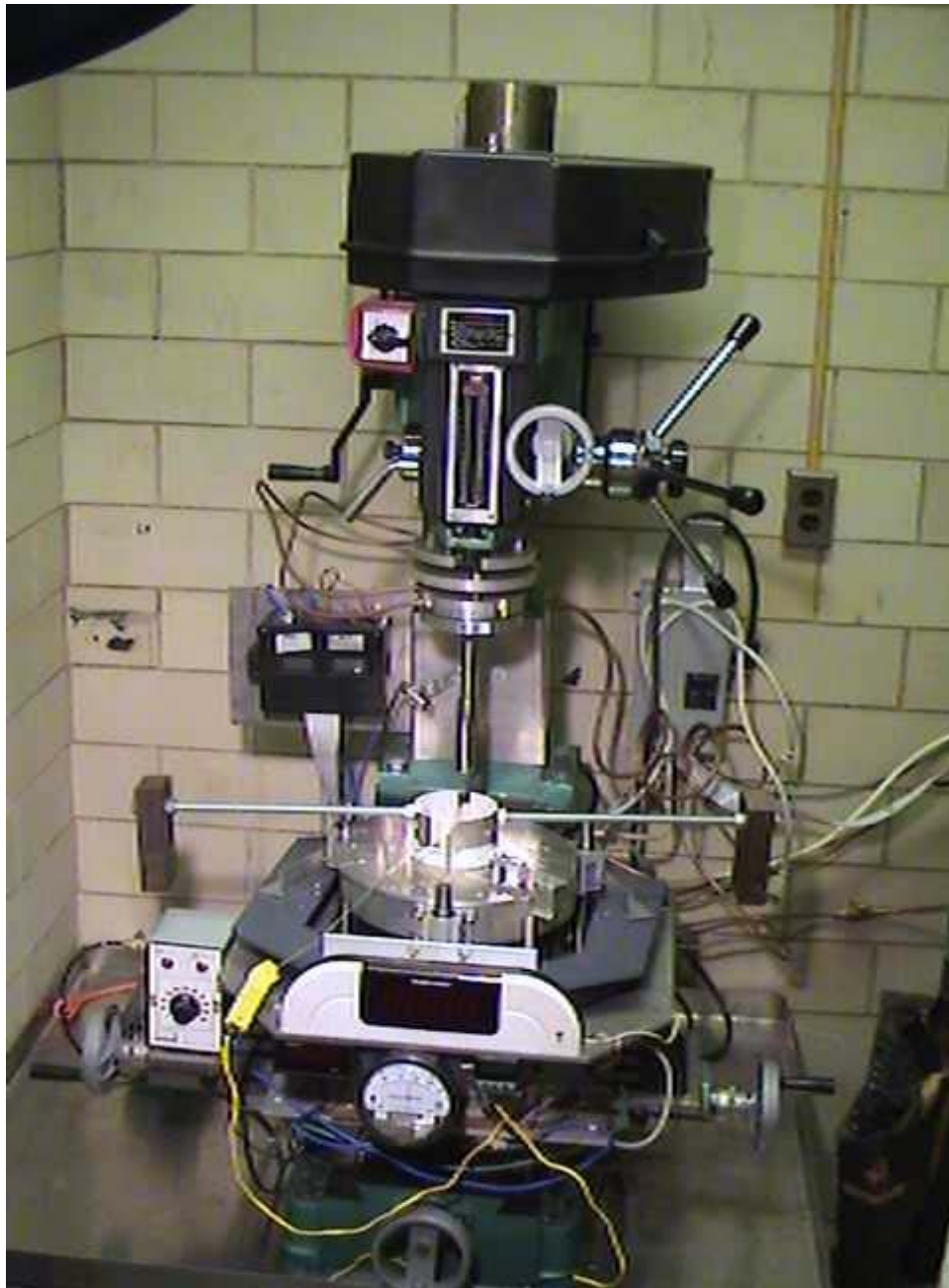
Figure 2.20: Assembled Zinc Pot Bearing Materials Tester

Chapter 3 - Material Wear Tester for Zinc-Pot Bearings

3.1 Improvement of Torque Strain Gage Beam

During operation of the WVU zinc pot bearing materials tester it was observed that the output signal form the torque strain gage beam was insufficient to produce a reliable reading by the data acquisition computer program. The previous design used two 350Ω strain gages attached to each side of a 1/2 inch wide aluminum beam. This design produced a conversion constant of 0.0898 lb_f / mV.

In order to improve the output signal a new torque strain gage beam was designed. Four 120Ω strain gages were attached to a 6061-T6 aluminum beam. The four strain gages were wired in a bridge configuration with a 25Ω potentiometer for zero balancing. With the new design a conversion constant of 0.0103 lb_f /mV was obtained. A schematic of the torque strain gage beam can be seen in Figure 3.1.

3.75"

Torque Transfer Beam

1.75"

Strain Gages

1.5"

0.25"

2.25"

Mounting Holes

1.0"
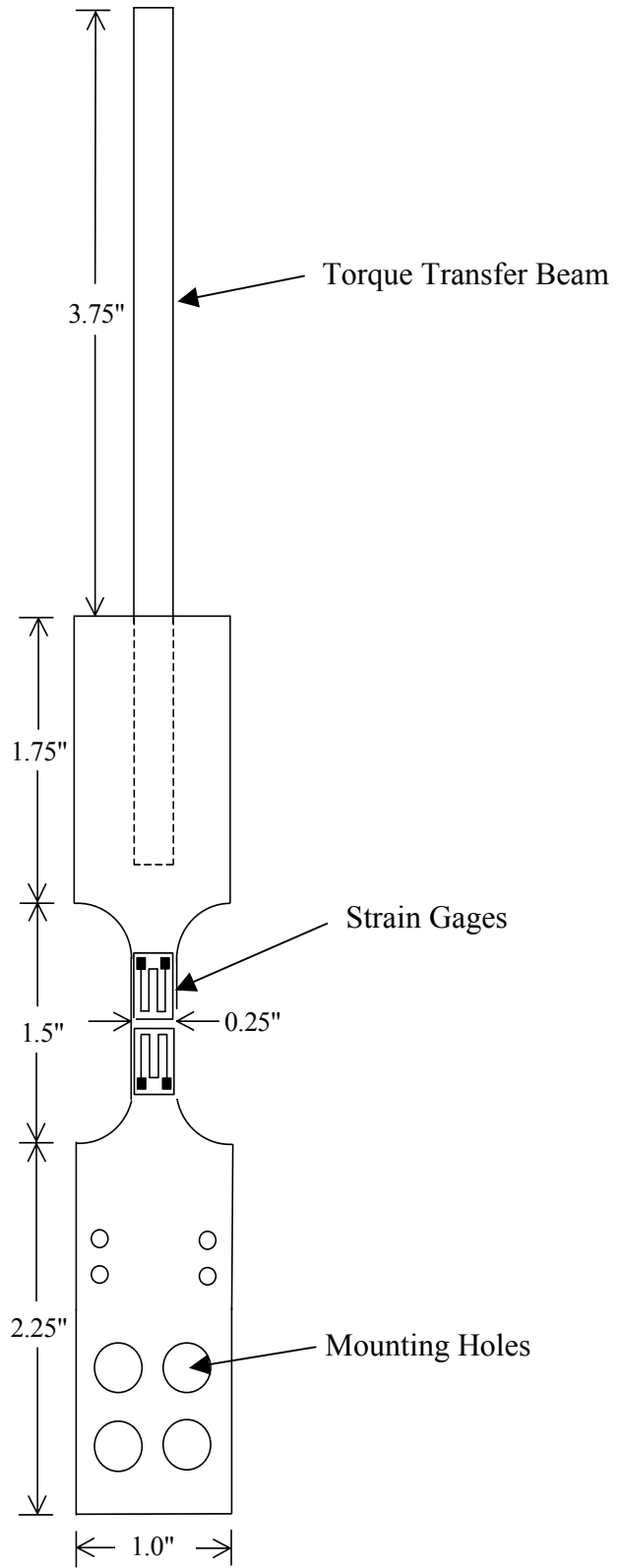
Figure 3.1: Improved Torque Strain Gage Beam

3.2 - Design of New Test Spindle

After performing tests using the spindle design described in Ryan Ware's thesis, the spindle began to wobble about its axis. The problem occurred at the junction of the Stainless Steel thin walled tubing and the 1-inch tubing. At this junction the fit between the two tubes was not secure. This indicated the need for a new test spindle.

The new spindle had to meet certain criteria, the first of which is that it had to be hollow so that a push rod could be inserted to remove the ball after a test was complete. The second criterion was that the hollow spindle allows a press fit attachment for the ball test specimen. With these criterion defined a new spindle was designed. The new design used a 3/4-inch O.D. piece of stainless steel tube with a 1/2-inch inside diameter for the main spindle. At the spindle end was a 3-inch long by 1-inch O.D. piece of stainless steel tubing attached. It is needed hold the 3.3-inch long 0.97-inch I.D. tubing, in to which the ball specimen is press fitted. The 1-inch O.D. tubing was pinned to the 3/4-inch tubing so that rotation was prevented during testing. A 1/2-inch thick by 5-inch radius aluminum disk was attached to the upper portion of the spindle for contact against a spring-loaded water-cooled disc of the same size. A diagram of the new spindle is shown in Figure 3.2.
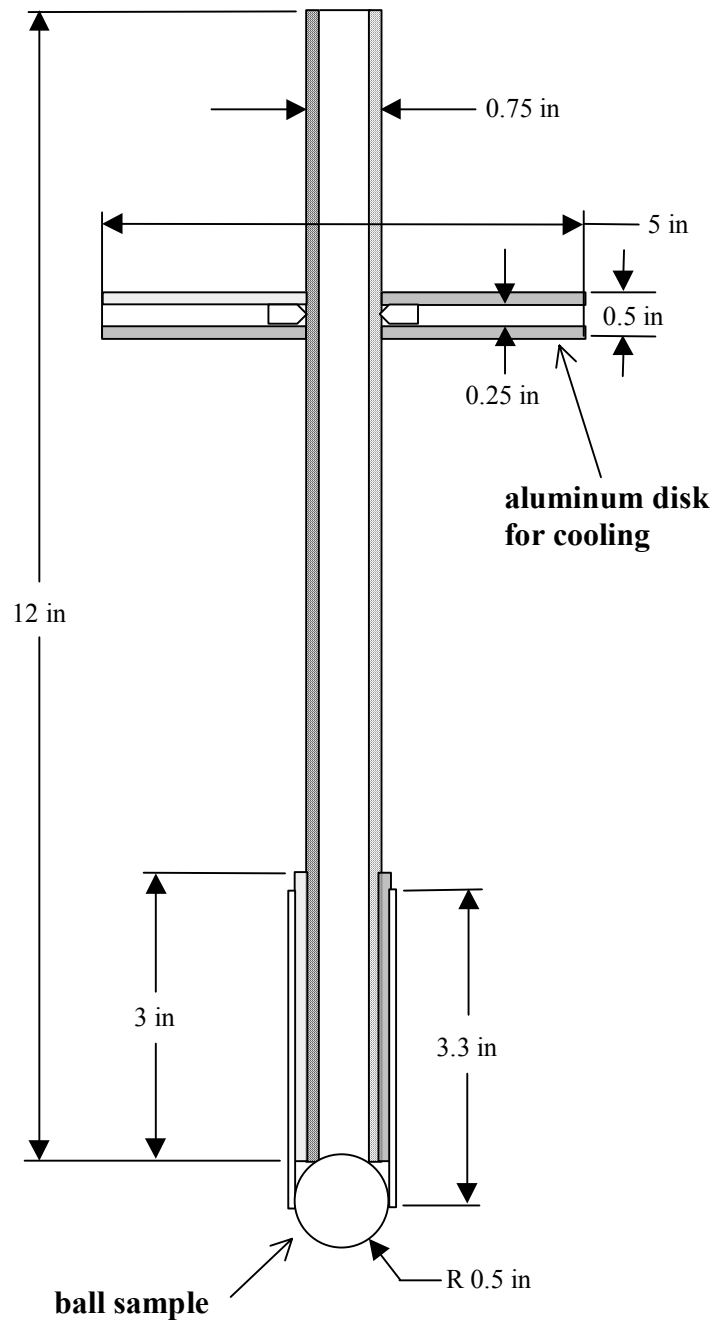
Figure 3.2: Rotating Spindle Design

3.3 - Zinc Pot Failure

During heating of the melting pot, its liner failed. After approximately 200 hours of operation the corrosive properties of the zinc produced a hole in the lining of the melting pot. The hole allowed the molten zinc to flow into the cavity between the pot lining and the outer shell where the heating elements are contained. This leak destroyed the pot.

A new melting pot was ordered with the same specifications as the old pot, with the addition of an electroplated chromed steel liner. The electroplated pot liner was painted with Boron Nitride Lubricoat to help further reduce the corrosion of the liner.

To minimize future melting pot problems, tin is now used in the pot in the place of zinc. The tin was placed in the melting pot to heat the zinc in the test cup to the desired test temperature. Tin has significantly lower corrosive properties than zinc and therefore will not attack the pot liner as rapidly. A tight fit prevents this coming in contact with the zinc inside the stainless steel cup holding the test specimen.

Chapter 4 - On-Line Data Acquisition Computer Program

4.1 Data Acquisition Computer Program

An Analog Devices RTI-800 Multifunction Input/Output Board was used to collect the four analog data signals produced by the zinc pot bearing tester during operation. A Quick Basic® computer program was written to run the RTI-800 board and store the collected signals in a database. The data collected was in the from of mV signals for the load, torque, RPM and temperature. With the use of an A/D converter the RTI-800 Board transforms the mV analog signals to 12-bit binary signals. This data was collected for 15 minutes with a sample being taken every 1 second. A 1 second interval was chosen since the RTI-800 Board is not capable of sample rates of less than 1 second. With the collected data saved to a database it was then possible to transform the data using Microsoft Excel® to determine the friction coefficient of the bearing materials tested. See Appendix A for a copy of the Quick Basic® computer program.

Chapter 5 - Friction Coefficient and Wear Data Analysis Procedure

5.1 Friction Coefficient Analysis Procedure

The four voltage data signals collected from the data acquisition computer program were saved to a database, which could be opened and saved as a Microsoft Excel® workbook. With the data in useable format it was then possible to calculate the sliding friction coefficient. The first step in this calculation procedure is to remove the gains from the voltage signal. This is done by dividing the collected voltage signal by its respective gain. Next, the voltage signal may be transformed to the proper units using the calibration constants found in Table 5.1. These constants were determined by calibrating the various strain gages, load cells, RPM meter and thermometer found on the WVU zinc pot bearing materials tester. A description of the calibration method and data collected can be found in Appendix B.

Table 5.1: Calibration Constants for Materials Tester

Instrument	Calibration Constant
Torque Strain Gage Beam	$0.031 \ lb_f / mV$
Load Cells	$0.4587 \ lb_f / mV$
Thermocouples	$1 \ ˚F / mV$
RPM Sensor	$0.2189 \ RPM / mV$

In order to remove any outlying data points from the data signal, an over-lap save method was employed. This method uses a moving average of the data to arrive at a new data point by averaging four data points together for a new point and saving the last three points used in the average for the next averaged point. This averaging procedure was used for all of the 900 data points collected during the friction coefficient test.

Because the ball rests on the seat at a 45° contact angle, the actual surface contact force is increased to $F_{contact} = 2(F_{load}*\sin45^o) = F_{load}*\sqrt{2}$. The friction torque at a moment

arm r_c = 1/2-inch*sin(45°) = 1/4*√2 = 0.3535-inches. The strain gage moment arm ℓ_{gage}

= 6.75-inch. With the data converted and averaged, the friction coefficient can now be

calculated using the following formula [13]:

$$\mu_F = \frac{F_{gage}*(\ell_{gage} = 6.75\,inch)}{F_{contact}*(r_c = 1/4*\sqrt{2}\,inch)} = \frac{13.5*F_{gage}}{F_{load}} \qquad \textbf{(5.1)}$$

The Friction Power dissipation rate, for the ball/seat system is the product of

ball/seat load, contact velocity and friction coefficient. Using the following formula gives

wear rate as a function of the friction power dissipation rate, which can be determined for

each test.

$$Friction\ Power = V_c * F_{load} * \sqrt{2} * \mu_f \qquad \textbf{(5.2)}$$

From experiments performed at constant contact pressure, wear is a linear function of

time and the square root of contact velocity. But at constant velocity it is proportional to

contact pressure squared, P_c^2. Therefore wear rate is proportional to power loading

equals P_c^2 (psi) * $\sqrt{V_c}$ (inch/sec) = $lb_f^2/(inch^{3/2} * sec^{1/2})$

5.2 Wear Analysis Procedure

The wear of the various test materials was determined by measuring the seat

material lost over a length of time at a prescribed set of test conditions. In order to

determine the loss of material, the average initial horizontal seat width W_i was measured

before starting the wear test, using an optical magnifier with a measurement scale inside.

The 6X optical magnifier was capable of measuring to the nearest 0.1-mm. The seat

width measurements were taken in four locations, North, South, East and West, as seen in Figure 5.1. These four measurements were then averaged to arrive at an average seat width, W_i.
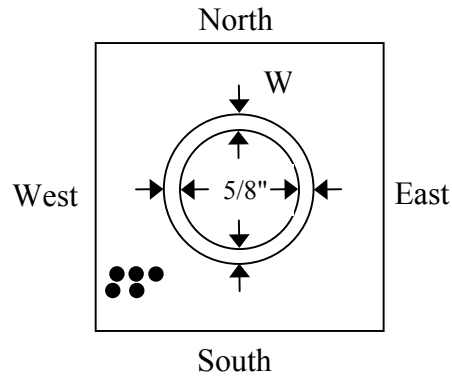
Figure 5.1: Measurement Locations on Seat Specimen

To obtain the amount of material lost from the sloped seat, a wear depth must be determined. This is done by dividing the average gain in seat width, $(W_f - W_I) = \Delta W$, by the square root of 2 as seen in the following formula.

$$WearDepth = \frac{\Delta W}{\sqrt{2}} \qquad \textbf{(5.3)}$$

This depth accounts for the loss of material on the 45˚ sloped seat, which can be seen in Figure 5.2.
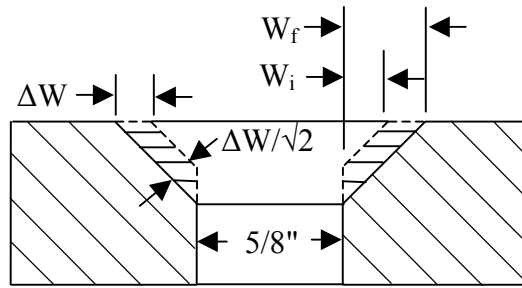
Figure 5.2: Wear Location of Seat Specimen

Next, the actual seat area was calculated using the seat width, W_i, by the following

$$A_{seat} = \frac{\pi}{4}((5/8"+2*W_i)^2 - (5/8")^2)*\sqrt{2}$$

formula.

(5.4)

Multiplying this initial actual seat area by the wear depth provides the seat material lost.

The average wear rate was calculated with the use of the wear depth and test duration.

$$Wear\ Rate = \left(\frac{\Delta W}{\sqrt{2}}\right)/t \qquad \textbf{(5.5)}$$

Chapter 6 - Wear and Friction Coefficient Results

6.1 Material Test Conditions

The materials tested for this project were selected by attendees of the Spring 2002 Conference meeting held at Oak Ridge National Laboratory. Most of these materials have been tested at WVU using contact pressures and velocities corresponding to average steel mill galvanizing line operating conditions. Figure 6.1 shows the relationship between contact velocity, V_c, and RPM of the WVU zinc pot bearing tester. Figure 6.2 shows the relationship between ball/seat pressure and spindle load. Both of these Figures are based on an average 45° contact angle of a 1-inch diameter ball, with a mean seat contact diameter of 0.707-inches. Because of the 5/8-inch diameter hole in the center, the projected seat area equals 0.171-inch^2. In both of these Figures are indicated the corresponding operating conditions at Weirton Steel galvanizing lines 3, 4, and 5. Most of tests were run with a contact pressure, P_c, and a contact velocity, V_c, corresponding to those used on line 3 and 4.
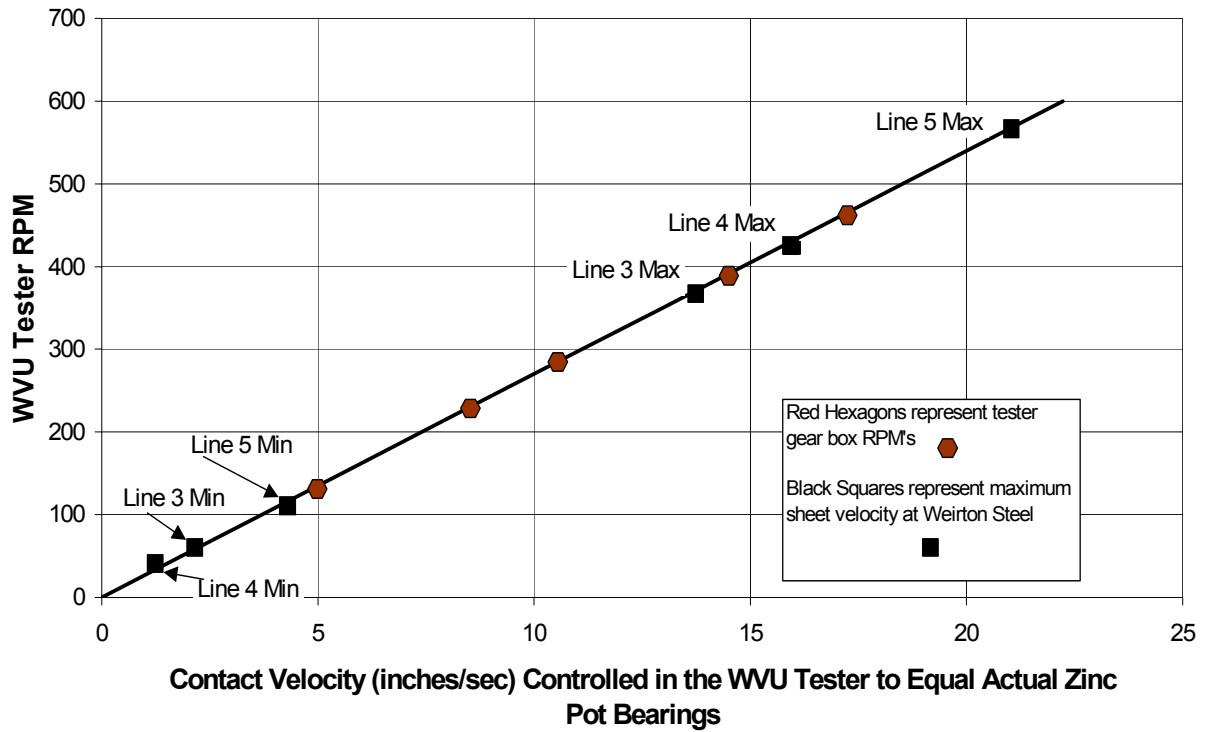
Figure 6.1: Contact Velocity as a Function of Bearing Tester RPM with Symbols Indicating Typical Contact Velocities Employed at Weirton Steel
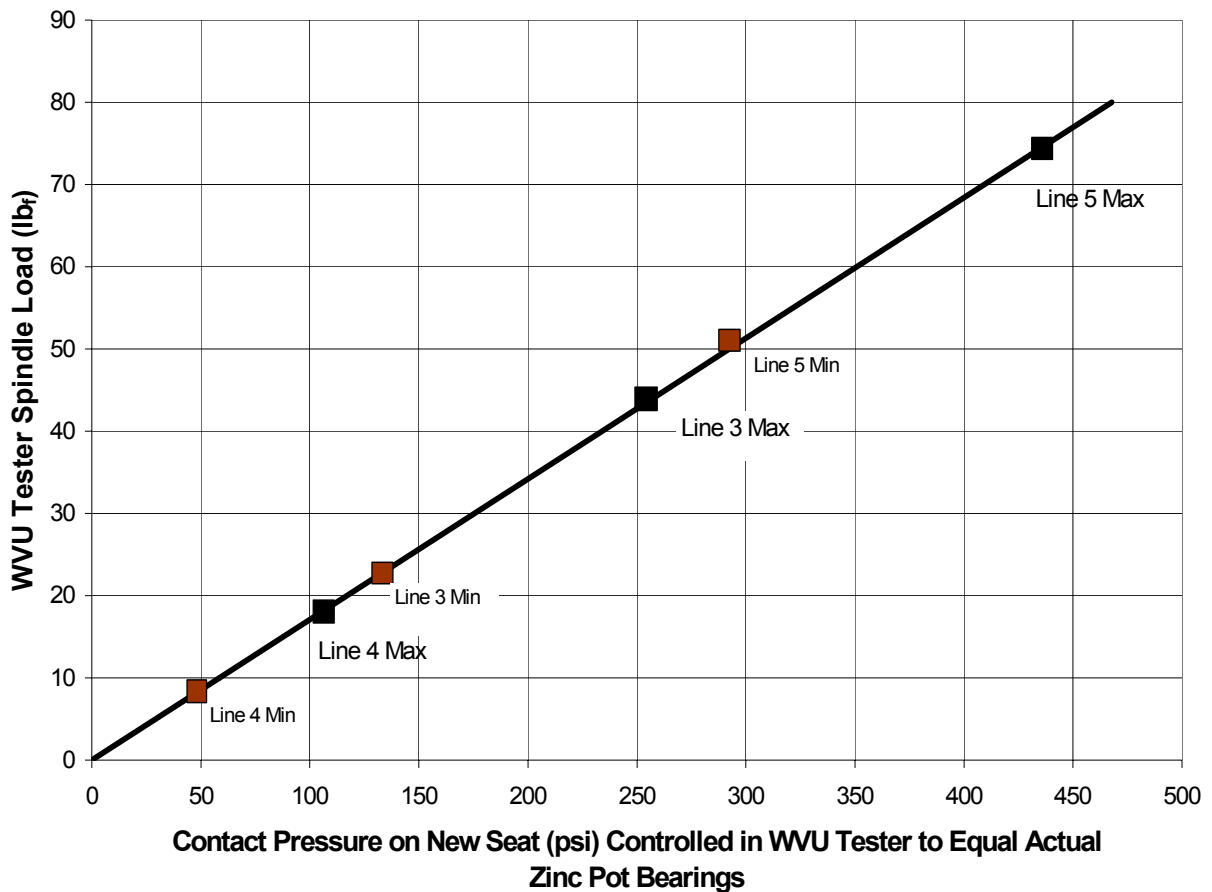
Figure 6.2: Contact Pressure as a Function of Spindle Load with Symbols Indicating Typical Contact Pressures Used at Weirton Steel

6.2 Test Samples Sources

Several industries provided test samples at no cost to WVU. Their contributions to this project are highly appreciated. Mike Brennan of Praxair Surface Technologies provided the Stellite #6 weld overlay and the laser-clad tungsten carbide ball and seat specimens. The MSA 2012 ball and seat specimens were provided by Mark Bright of Metaullics Molten Metal Systems. In addition, Metaullics provided 1-inch hemispherical ball samples of MSA 2020 for testing. Ed Dean of Vesuvius McDanel provided ceramic seats for testing and Vinod Sikka provided both Stellite #6 and ORNL-4.

6.3 Wear Tests in Water

To determine the effects of contact velocity and initial contact pressure on material wear, a series of water tests were conducted. The first of these was performed with a Stainless Steel ball specimen on a Stainless Steel seat specimen to determine the wear rate as a function of time at various velocities. Shown in Figure 6.3 are the results from this test. The results showed that wear rate is linear with time.
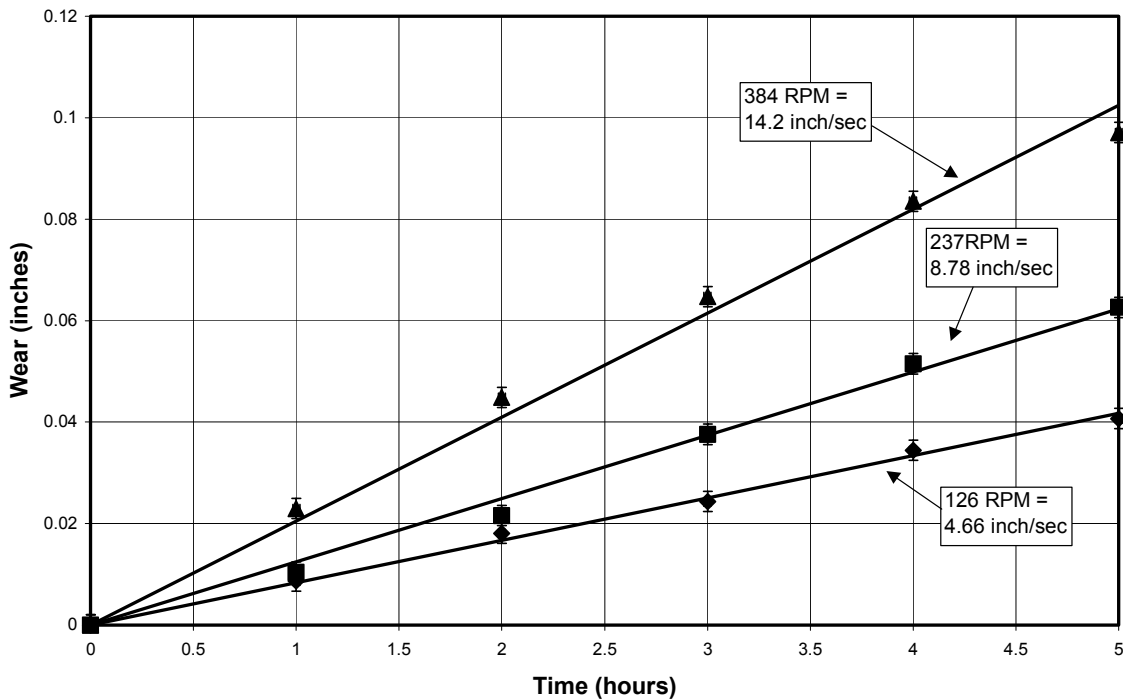
Figure 6.3: Wear of Stainless Steel on Stainless Steel as a Function of Time at an Initial Contact Pressure of 100 psi and Various Contact Velocities in Water

The wear rate as a function of initial contact pressure was a determined using a Stainless Steel ball specimen on a Stainless Steel seat specimen. These tests were performed at various RPM's. Figure 6.4 shows that the wear rate is a quadratic of contact pressure. In order to account for this non-linearity a curve fit was conducted, which

determined that the wear rate is equal to $C*P_c^2 * \sqrt{V_c}$. Where C is a proportionality

constant. This relation is shown in Figure 6.5.
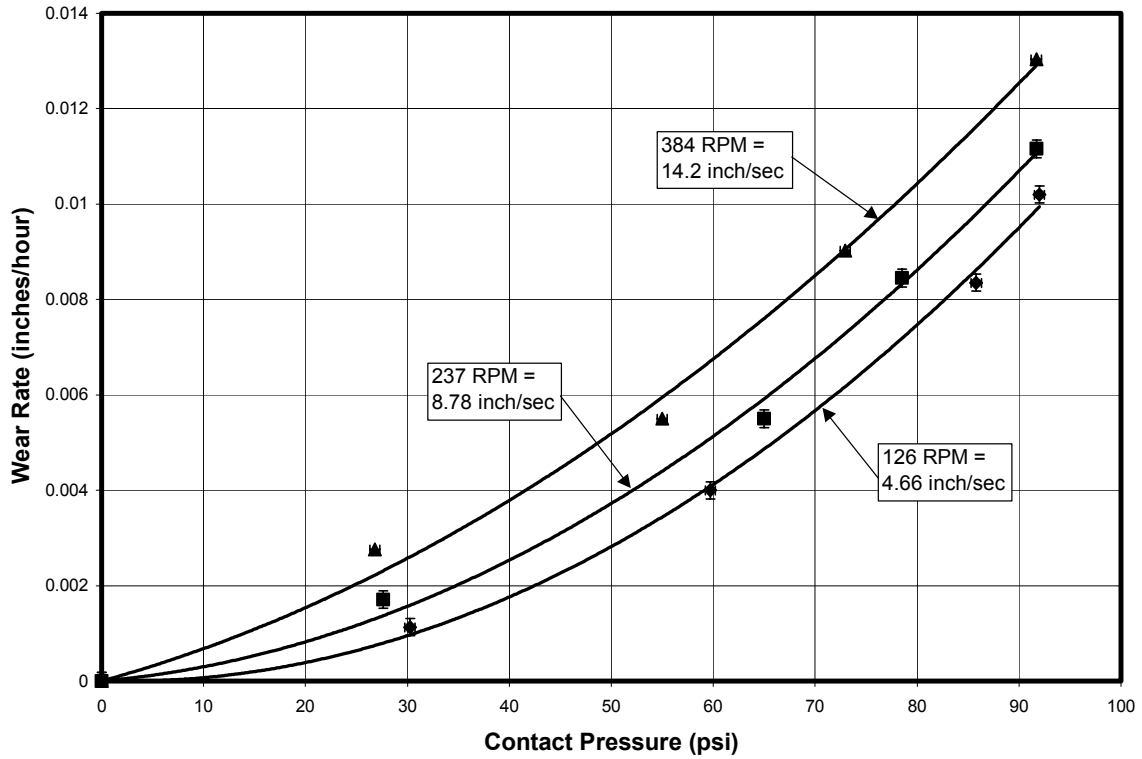
Figure 6.4: Wear as a Function of Contact Pressure for Stainless Steel on Stainless Steel at Various Contact Velocities in Water
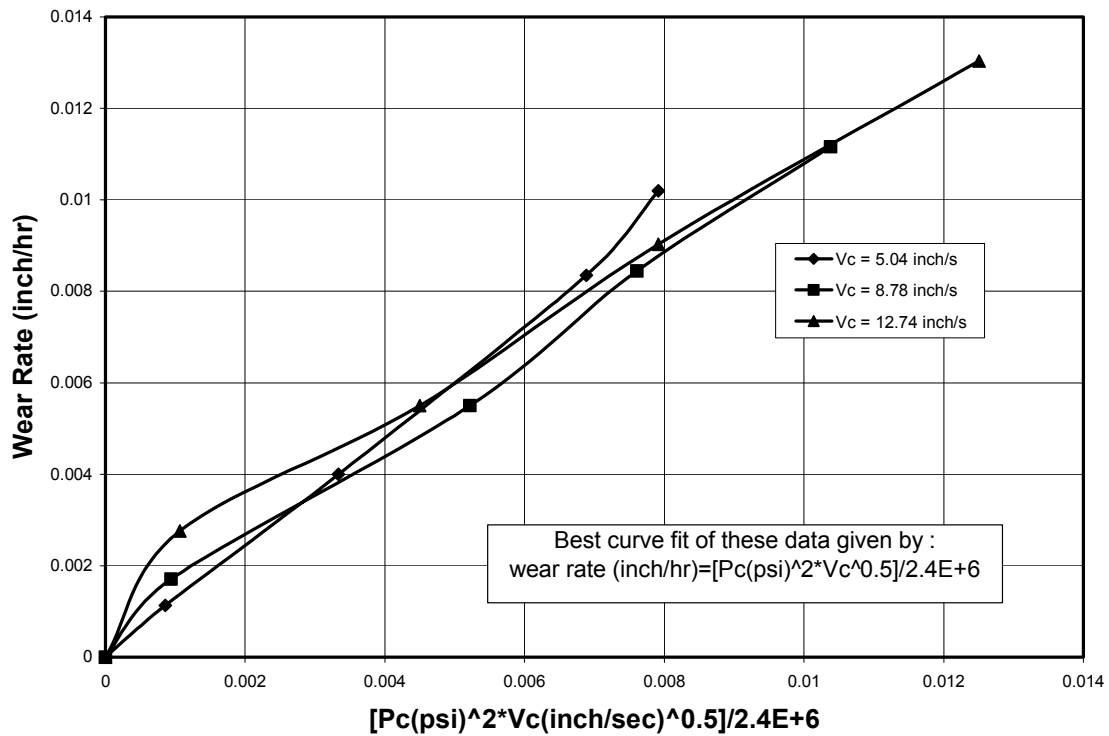
Figure 6.5: Wear Rate of Stainless Steel on Stainless Steel in Water and Curve Fitted as a Function of Contact Pressure and Velocity

A Stellite #6 ball specimen on a Stellite #6 seat specimen were also tested in water to determine if wear rate as a function of time remained linear. As shown in Figure 6.6, the wear rate remained linear with time for Stellite #6.
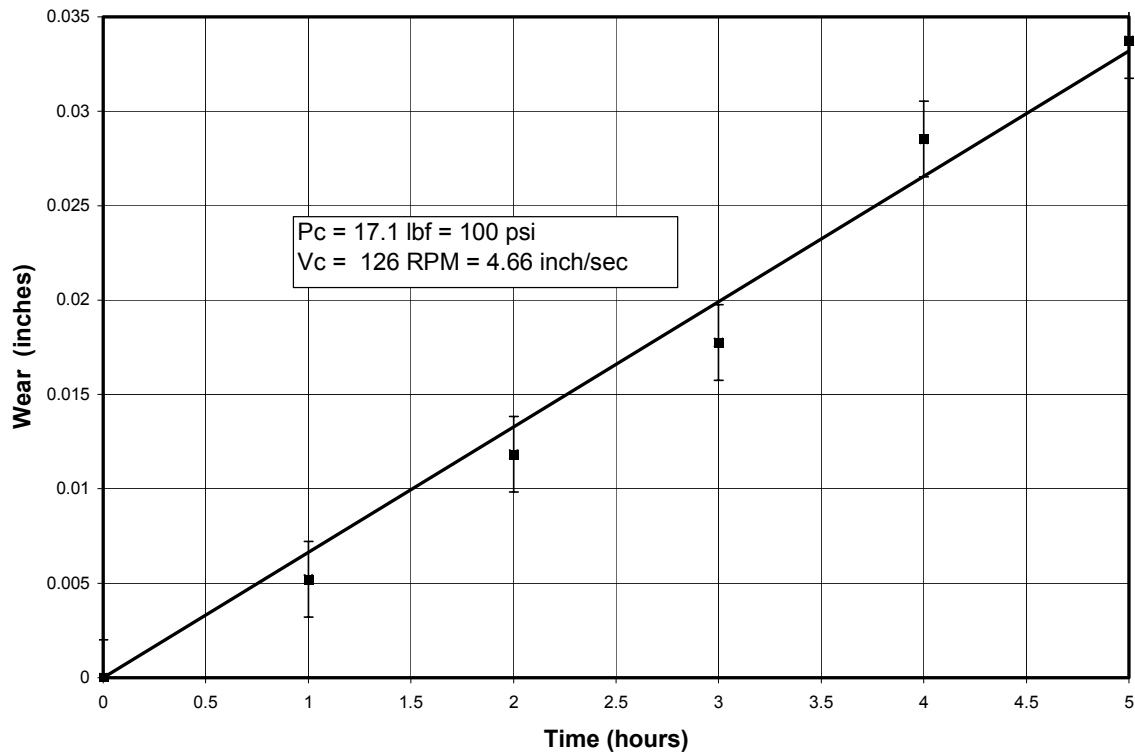
**Figure 6.6: Wear of Stellite #6 on Stellite #6 as a Function of Time in Water
at a Contact Pressure of 100 psi and a Contact Velocity of 4.56 inches/sec**

A test was also performed to determine the effects of contact pressure on the wear rate of a Stellite #6 ball specimen on a Stellite #6 seat specimen. The wear rate as a function of contact pressure is non-linear, as shown in Figure 6.7. A curve fit was performed for this material that determined that the wear rate was equal to $C*P_c^2 * \sqrt{V_c}$, as shown in Figure 6.8.
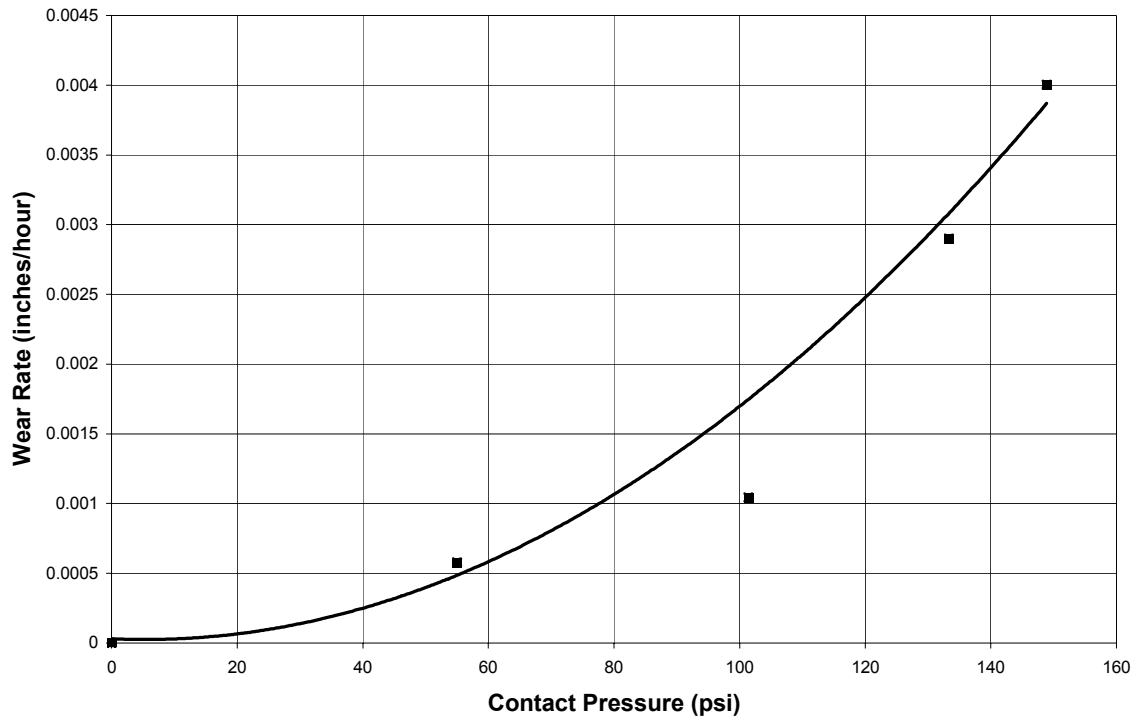
Figure 6.7: Wear as a Function of Contact Pressure for a Stellite #6 Ball on a Stellite #6 Seat at a Contact Velocity of 4.66 inches/sec in Water
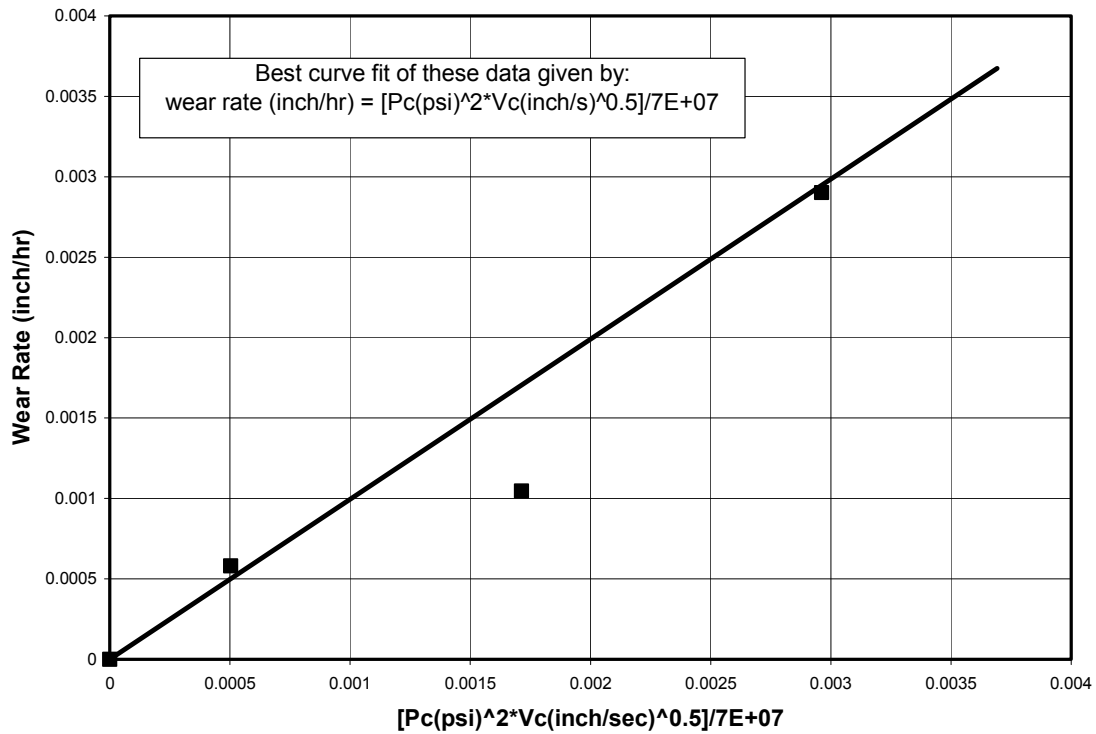
Figure 6.8: Wear Rate of Stellite #6 on Stellite #6 in Water and Curve Fitted as a Function of Contact Pressure and Velocity

The above cold water tests for combinations of stainless steel on stainless steel and Stellite #6 on Stellite #6 showed that the wear rate is linear with time and non-linear with respect to contact pressure.

6.4 Hot Zinc Tests

Hot zinc tests were performed in molten zinc to determine the sliding friction coefficient and wear rate of various material combinations. The seat widths were measured before and after each wear test and the friction coefficient was determined during the wear test. Each sample was oxidized before each test by placing it in close

proximity to the molten tin bath at approximately 860°F. Figures 6.9 through 6.15 show

the results of the friction coefficient tests performed on various material combinations.

Test Conditions:
Ball/Seat Load = 35 lb$_f$
Contact Pressure = 268 psi
RPM = 280
Contact Velocity = 10.4 inches/sec
Temperature = 859 °F
Measured Avg. Friction Coefficient = 0.0793
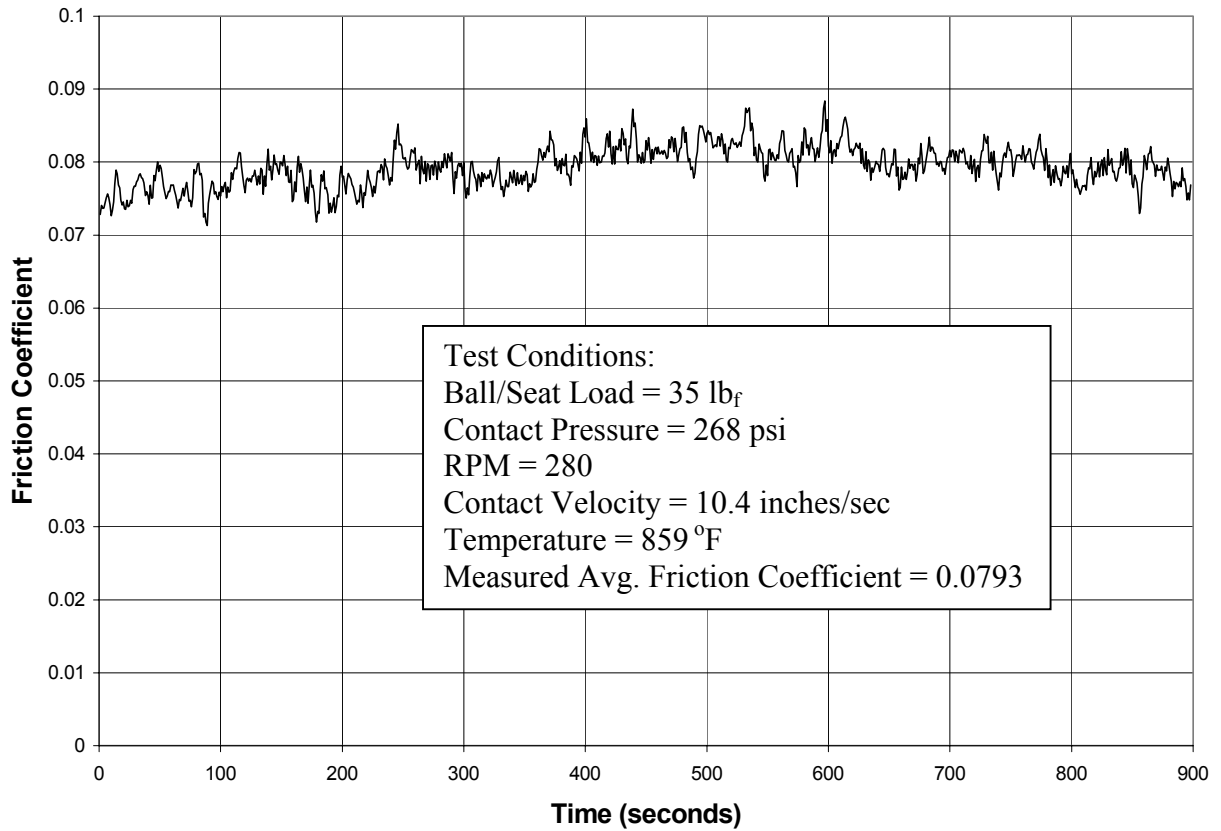
**Figure 6.9: Friction Coefficient of a MSA 2012 Ball on a
Stellite #6 Seat as a Function of Time**
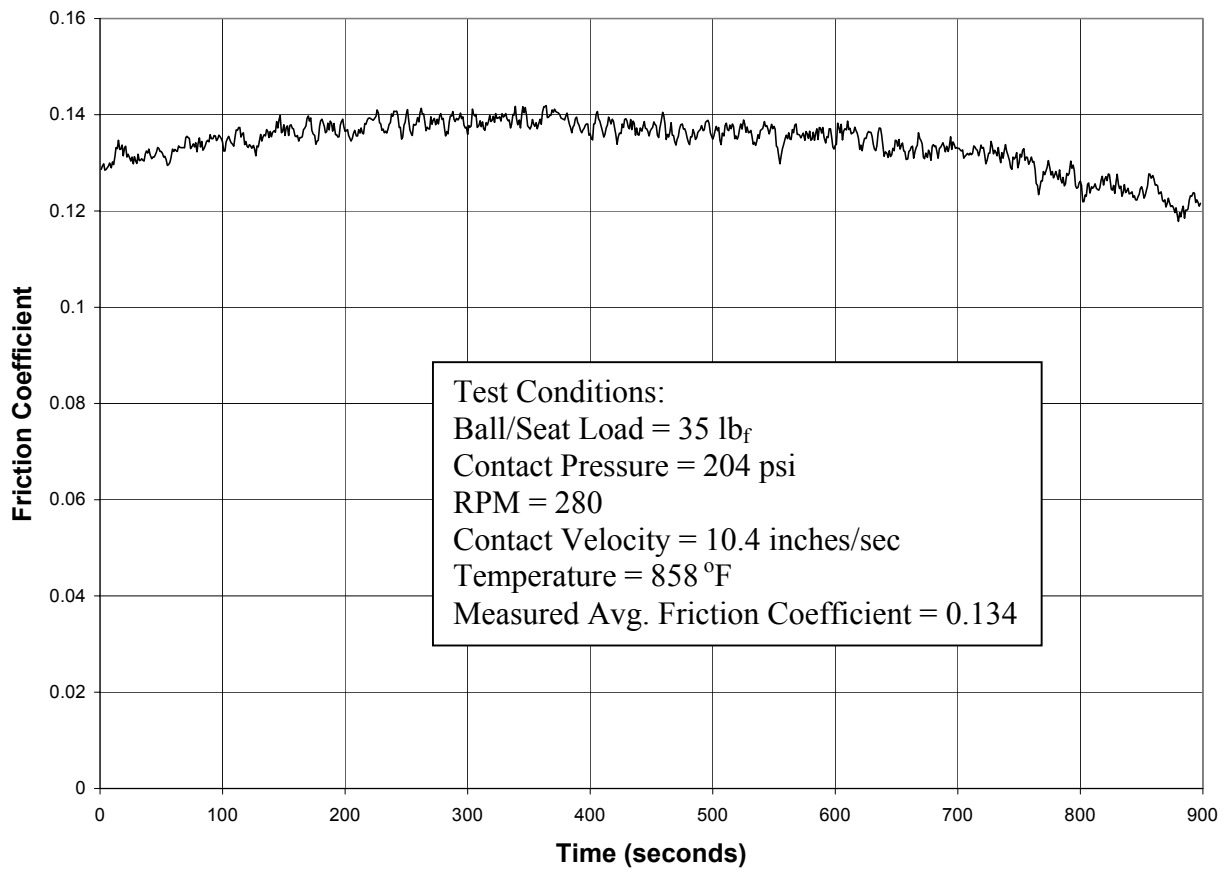
Figure 6.10: Friction Coefficient of a MSA 2012 Ball on a Laser-Clad Tungsten Carbide Seat as a Function of Time

Test Conditions:
Ball/Seat Load = 35 lb$_f$
Contact Pressure = 198 psi
RPM = 280
Contact Velocity = 10.4 inches/sec
Temperature = 859 ^{o}F
Measured Avg. Friction Coefficient = 0.135
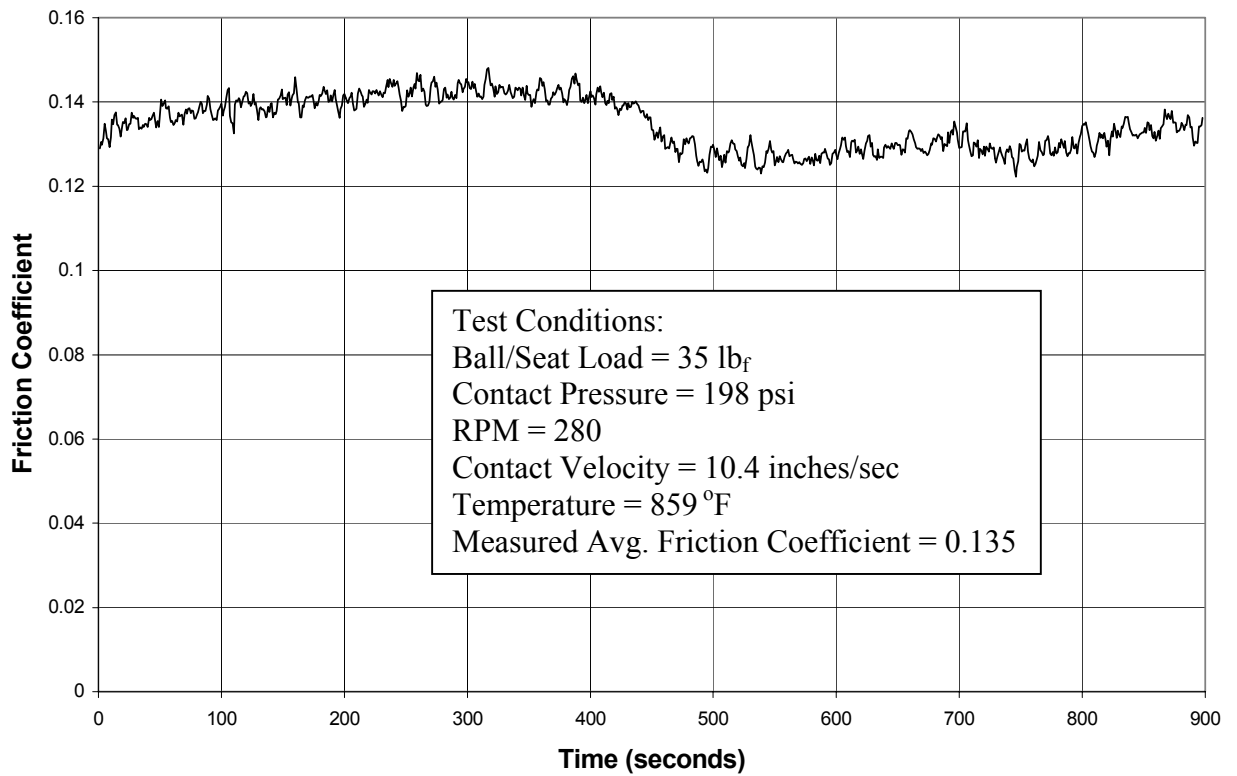
**Figure 6.11: Friction Coefficient of a MSA 2020 Ball on a
Laser-Clad Tungsten Carbide Seat as a Function of Time**
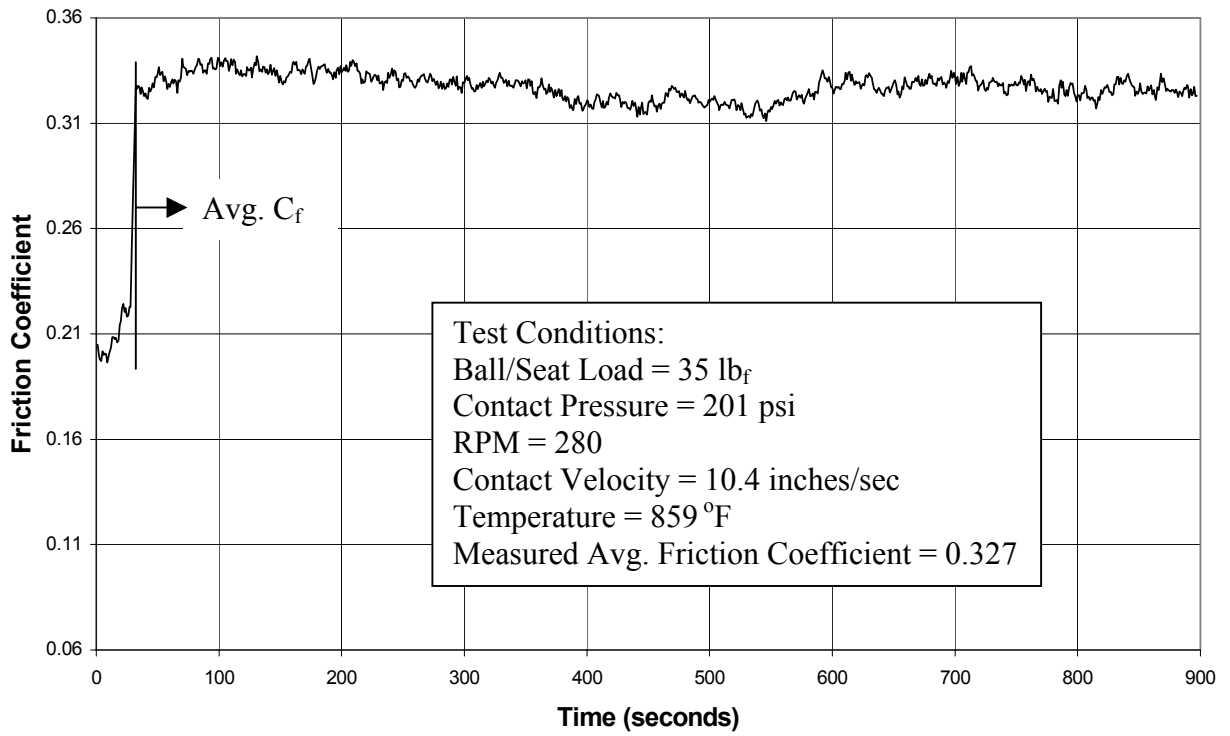
**Figure 6.12: Friction Coefficient of a MSA 2020 Ball on a
MSA 2012 Seat as a Function of Time**
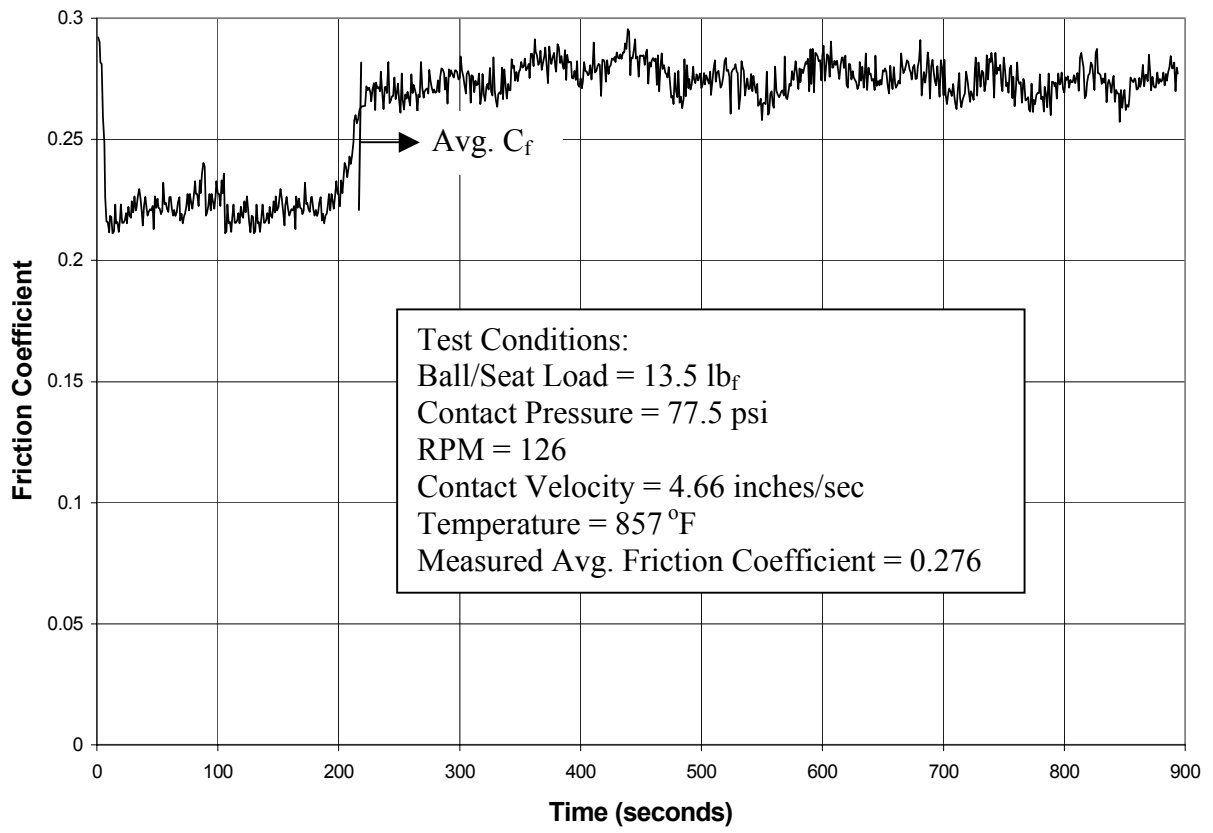
**Figure 6.13: Friction Coefficient of a MSA 2012 Ball on a
MSA 2012 Seat as a Function of Time**

58

Test Conditions:
Ball/Seat Load = 35 lb_f
Contact Pressure = 201 psi
RPM = 280
Contact Velocity = 10.4 inches/sec
Temperature = 858 ^{o}F
Measured Avg. Friction Coefficient = 0.126
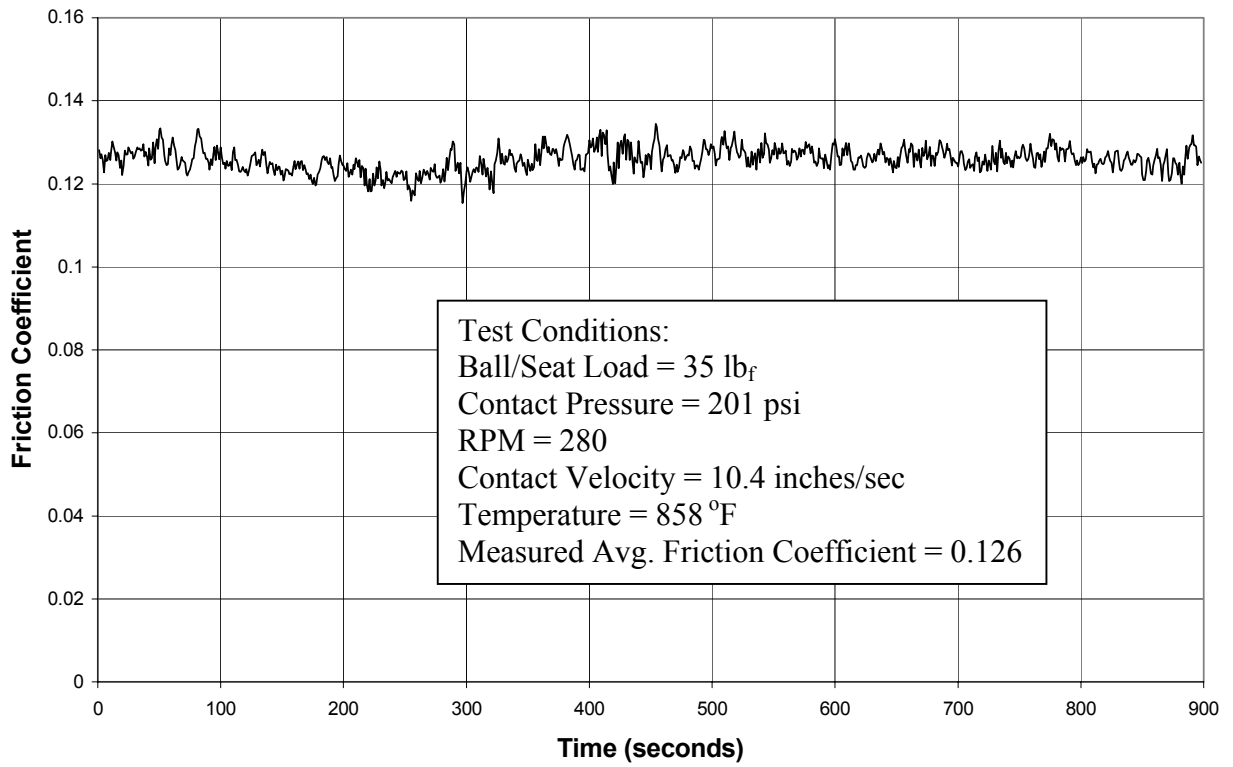
**Figure 6.14: Friction Coefficient of a Stellite #6 Ball on a
MSA 2012 Seat as a Function of Time**
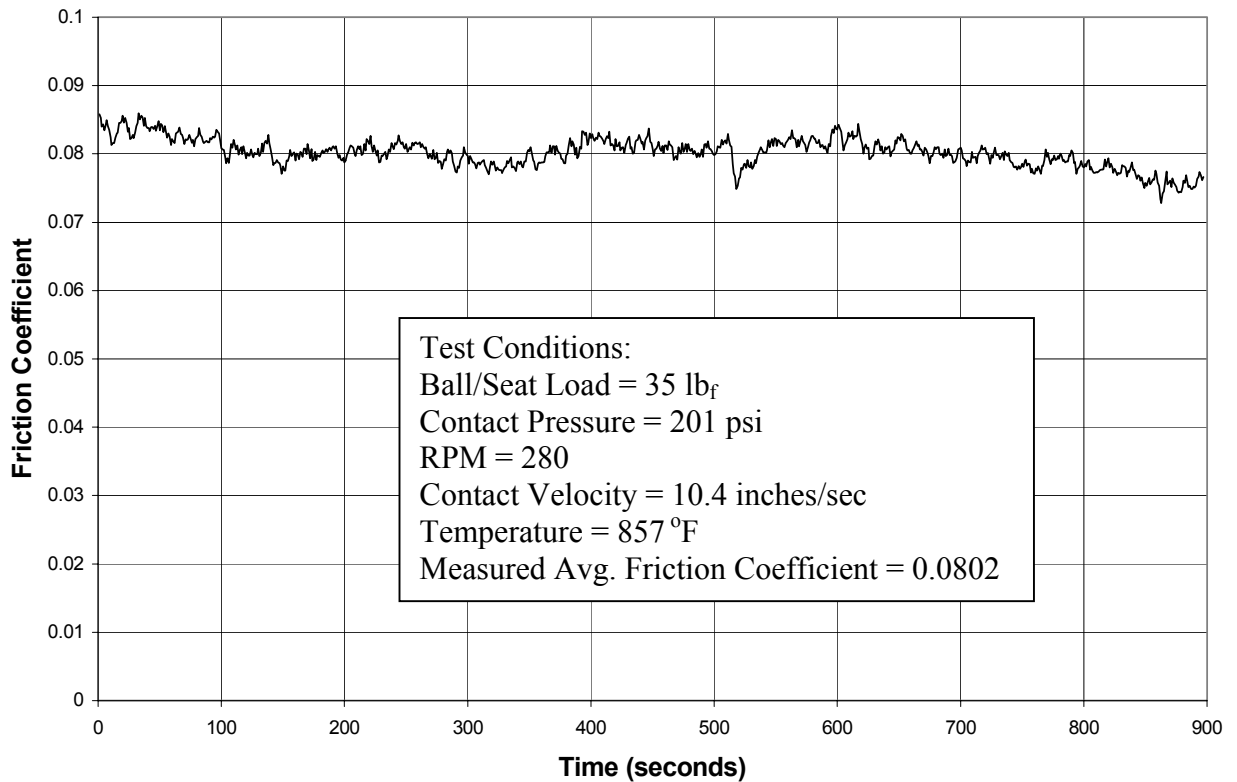
Figure 6.15: Friction Coefficient of a Laser-Clad Tungsten Carbide Ball on a MSA 2012 Seat as a Function of Time

The wear rates of various material combinations were determined by measuring the increase in seat width at four locations, North, South, East and West. With this information the wear rate and initial and final horizontal seat areas were determined. Table 6.1 shows the wear rate of various material combinations along with the test specifications.

Table 6.1: Wear Rate and Friction Power of Various Material Combinations

Stationary Ball Seat Material with 5/8" hole	Stellite #6 Weld Overlay
Spindle Ball End Material	Laser Clad - Tungsten Carbide
Test Date	July 7, 2002
Contact Velocity, V_c = RPM / 27 = 126 / 27	4.66 in/sec
Initial Contact Pressure, P_c = Load / A_{hi} = 10.5lb_f / A_{hi}	60.3 psi
Test Duration, t	20 hours
Average Cup Test Temperature	870 ºF
Horizontal Seat Width, W_{hi} and W_{hf}	0.0787 in. - 0.119 in.
Initial Horizontal Seat Area, A_{hi} = π (r_i^2 - 5/16^2)	0.174 in^2
Final Horizontal Seat Area, A_{hf} = π (r_f^2 - 5/16^2)	0.278 in^2
Average Wear Rate, (r_f - r_i)/(t*2$^{1/2}$)	0.00143 in/hr
Friction Coefficient, μ_f	0.358
Friction Power = V_c*F_θ = V_c*Load*μ_f	17.5 (lb_f*in)/sec

*subscript i indicates initial at start of test, subscript f indicates final at end of test

Stationary Ball Seat Material with 5/8" hole	Stellite #6 Weld Overlay
Spindle Ball End Material	MSA 2012
Test Date	November 12, 2002
Contact Velocity, V_c = RPM / 27 = 280 / 27	10.4 in/sec
Initial Contact Pressure, P_c = Load / A_{hi} = 35lb_f / A_{hi}	268 psi
Test Duration, t	5.25 hours
Average Cup Test Temperature	859 ºF
Horizontal Seat Width, W_{hi} and W_{hf}	0.0605 in. - 0.0778 in.
Initial Horizontal Seat Area, A_{hi} = π (r_i^2 - 5/16^2)	0.130 in^2
Final Horizontal Seat Area, A_{hf} = π (r_f^2 - 5/16^2)	0.172 in^2
Average Wear Rate, (r_f - r_i)/(t*2$^{1/2}$)	0.00232 in/hr
Friction Coefficient, μ_f	0.0793
Friction Power = V_c*F_θ = V_c*Load*μ_f	28.9 (lb_f*in)/sec

Stationary Ball Seat Material with 5/8" hole	Laser Clad - Tungsten Carbide
Spindle Ball End Material	MSA 2012
Test Date	November 12, 2002
Contact Velocity, V_c = RPM / 27 = 280 / 27	10.4 in/sec
Initial Contact Pressure, P_c = Load / A_{hi} = 35lb_f / A_{hi}	204 psi
Test Duration, t	5.25 hours
Average Cup Test Temperature	858 ºF
Horizontal Seat Width, W_{hi} and W_{hf}	0.0778 in. - 0.0851 in.
Initial Horizontal Seat Area, $A_{hi} = \pi (r_i^2 - 5/16^2)$	0.172 in^2
Final Horizontal Seat Area, $A_{hf} = \pi (r_f^2 - 5/16^2)$	0.190 in^2
Average Wear Rate, $(r_f - r_i)/(t*2^{1/2})$	0.000994 in/hr
Friction Coefficient, μ_f	0.134
Friction Power = $V_c*F_\theta = V_c*Load*\mu_f$	48.8 (lb_f*in)/sec

Stationary Ball Seat Material with 5/8" hole	Laser Clad - Tungsten Carbide
Spindle Ball End Material	MSA 2020
Test Date	November 11, 2002
Contact Velocity, V_c = RPM / 27 = 280 / 27	10.4 in/sec
Initial Contact Pressure, P_c = Load / A_{hi} = 35lb_f / A_{hi}	198 psi
Test Duration, t	6.1 hours
Average Cup Test Temperature	856 ºF
Horizontal Seat Width, W_{hi} and W_{hf}	0.0797 in. - 0.0915 in.
Initial Horizontal Seat Area, $A_{hi} = \pi (r_i^2 - 5/16^2)$	0.176 in^2
Final Horizontal Seat Area, $A_{hf} = \pi (r_f^2 - 5/16^2)$	0.206 in^2
Average Wear Rate, $(r_f - r_i)/(t*2^{1/2})$	0.00137 in/hr
Friction Coefficient, μ_f	0.135
Friction Power = $V_c*F_\theta = V_c*Load*\mu_f$	49.1 (lb_f*in)/sec

Stationary Ball Seat Material with 5/8" hole	MSA 2012
Spindle Ball End Material	MSA 2012
Test Date	September 11, 2002
Contact Velocity, V_c = RPM / 27 = 126 / 27	4.66 in/sec
Initial Contact Pressure, P_c = Load / A_{hi} = 13.5lb_f / A_{hi}	77.5 psi
Test Duration, t	17 hours
Average Cup Test Temperature	870 ºF
Horizontal Seat Width, W_{hi} and W_{hf}	0.0787 in. - 0.0866 in.
Initial Horizontal Seat Area, $A_{hi} = \pi (r_i^2 - 5/16^2)$	0.174 in^2
Final Horizontal Seat Area, $A_{hf} = \pi (r_f^2 - 5/16^2)$	0.194 in^2
Average Wear Rate, $(r_f - r_i)/(t*2^{1/2})$	0.000328 in/hr
Friction Coefficient, μ_f	0.276
Friction Power = $V_c*F_\theta = V_c*Load*\mu_f$	17.4 (lb_f*in)/sec

Stationary Ball Seat Material with 5/8" hole	MSA 2012
Spindle Ball End Material	MSA 2020
Test Date	November 1, 2002
Contact Velocity, V_c = RPM / 27 = 280 / 27	10.4 in/sec
Initial Contact Pressure, P_c = Load / A_{hi} = 35lb$_f$ / A_{hi}	201 psi
Test Duration, t	5.25 hours
Average Cup Test Temperature	859 ºF
Horizontal Seat Width, W_{hi} and W_{hf}	0.0787 in. - 0.0906 in.
Initial Horizontal Seat Area, $A_{hi} = \pi (r_i^2 - 5/16^2)$	0.174 in^2
Final Horizontal Seat Area, $A_{hf} = \pi (r_f^2 - 5/16^2)$	0.204 in^2
Average Wear Rate, $(r_f - r_i)/(t*2^{1/2})$	0.00159 in/hr
Friction Coefficient, μ_f	0.327
Friction Power = $V_c*F_\theta = V_c*Load*\mu_f$	119.0 (lb$_f$*in)/sec

Stationary Ball Seat Material with 5/8" hole	MSA 2012
Spindle Ball End Material	Stellite #6 Weld Overlay
Test Date	November 11, 2002
Contact Velocity, V_c = RPM / 27 = 280 / 27	10.4 in/sec
Initial Contact Pressure, P_c = Load / A_{hi} = 35lb$_f$ / A_{hi}	201 psi
Test Duration, t	5.25 hours
Average Cup Test Temperature	858 ºF
Horizontal Seat Width, W_{hi} and W_{hf}	0.0787 in. - 0.0866 in.
Initial Horizontal Seat Area, $A_{hi} = \pi (r_i^2 - 5/16^2)$	0.174 in^2
Final Horizontal Seat Area, $A_{hf} = \pi (r_f^2 - 5/16^2)$	0.194 in^2
Average Wear Rate, $(r_f - r_i)/(t*2^{1/2})$	0.00106 in/hr
Friction Coefficient, μ_f	0.126
Friction Power = $V_c*F_\theta = V_c*Load*\mu_f$	45.9 (lb$_f$*in)/sec

Stationary Ball Seat Material with 5/8" hole	MSA 2012
Spindle Ball End Material	Laser Clad - Tungsten Carbide
Test Date	November 2, 2002
Contact Velocity, V_c = RPM / 27 = 280 / 27	10.4 in/sec
Initial Contact Pressure, P_c = Load / A_{hi} = 35lb$_f$ / A_{hi}	201 psi
Test Duration, t	5.25 hours
Average Cup Test Temperature	857 ºF
Horizontal Seat Width, W_{hi} and W_{hf}	0.0787 in. - 0.101 in.
Initial Horizontal Seat Area, $A_{hi} = \pi (r_i^2 - 5/16^2)$	0.174 in^2
Final Horizontal Seat Area, $A_{hf} = \pi (r_f^2 - 5/16^2)$	0.231 in^2
Average Wear Rate, $(r_f - r_i)/(t*2^{1/2})$	0.00305 in/hr
Friction Coefficient, μ_f	0.0802
Friction Power = $V_c*F_\theta = V_c*Load*\mu_f$	29.2 (lb$_f$*in)/sec

Shown in Figure 6.16 are the average friction coefficients for the material combinations tested.
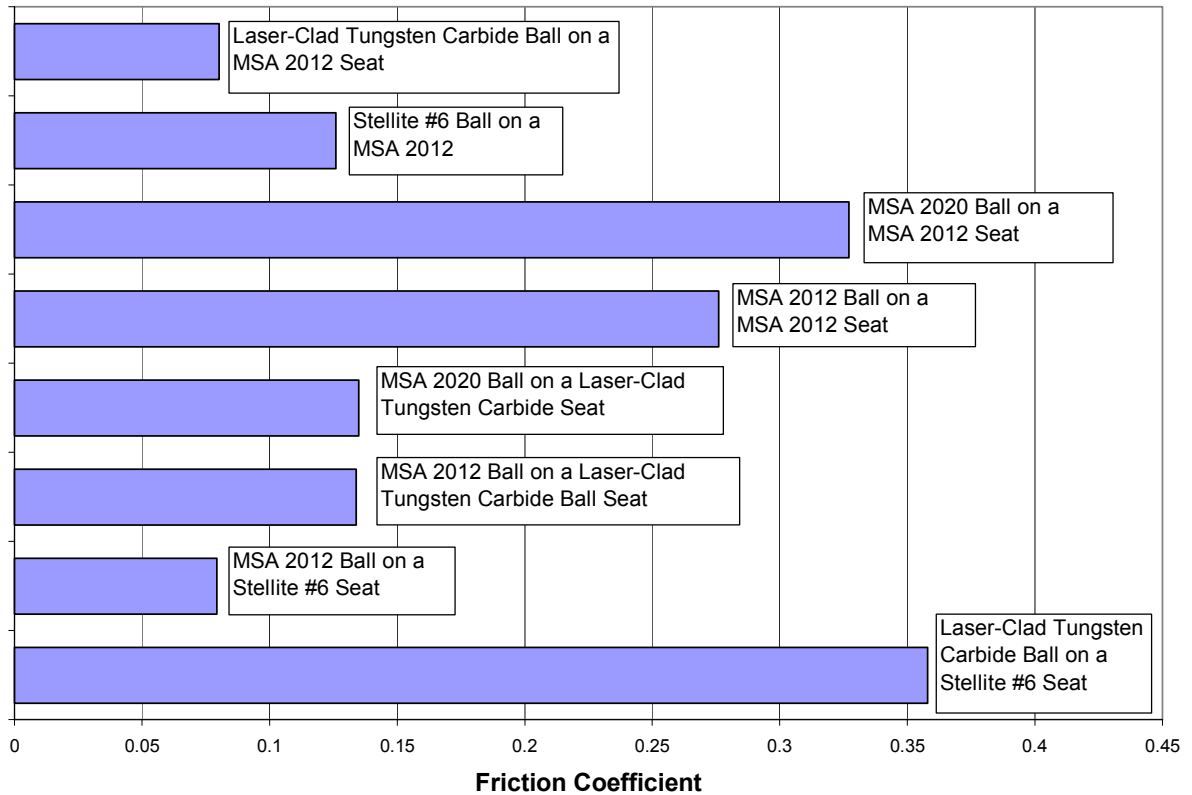
Figure 6.16: Average Friction Coefficients of Bearing Material Combinations

The friction power of each material combination was calculated using the average friction coefficient for that material in Equation 5.5. Figure 6.17 shows a comparison of the friction power for each material combination tested.
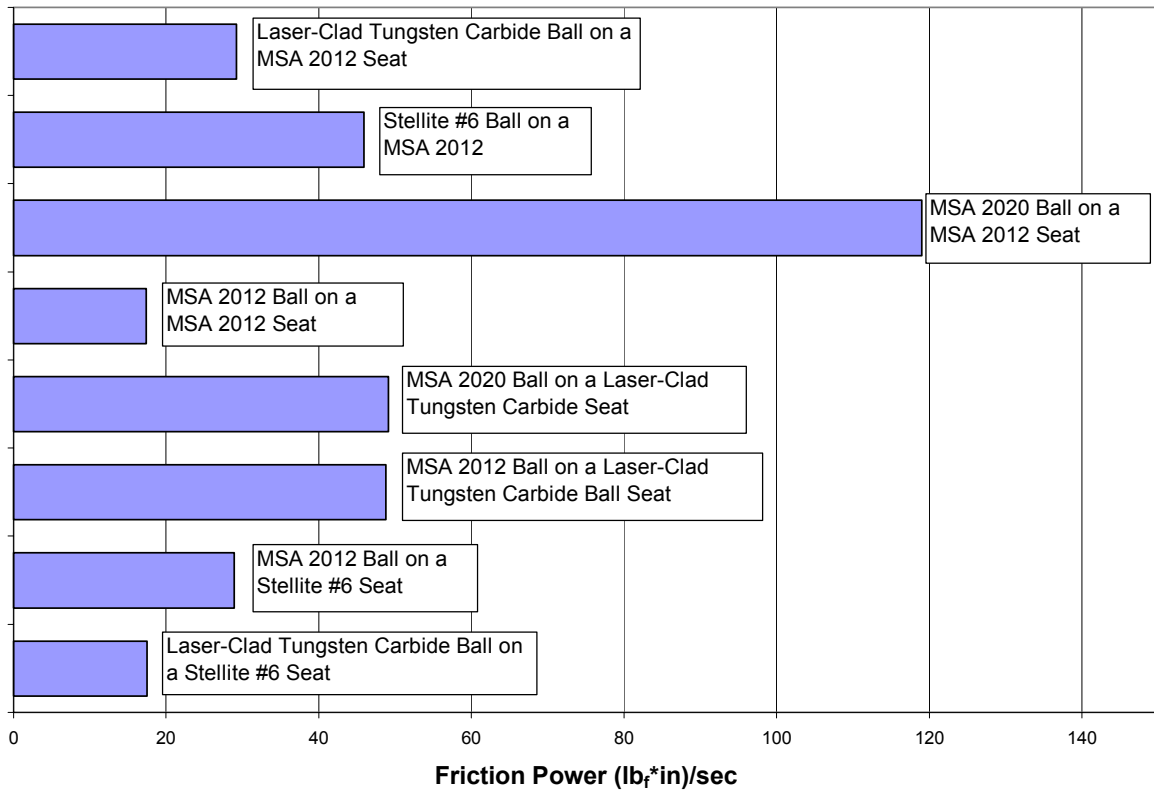
Figure 6.17: Friction Power of Bearing Material Combinations

A correlation between bearing loading power and wear rate was also constructed, shown in Figure 6.18. From this Figure it was concluded that the Laser-Clad Tungsten carbide seat lasted the longest.
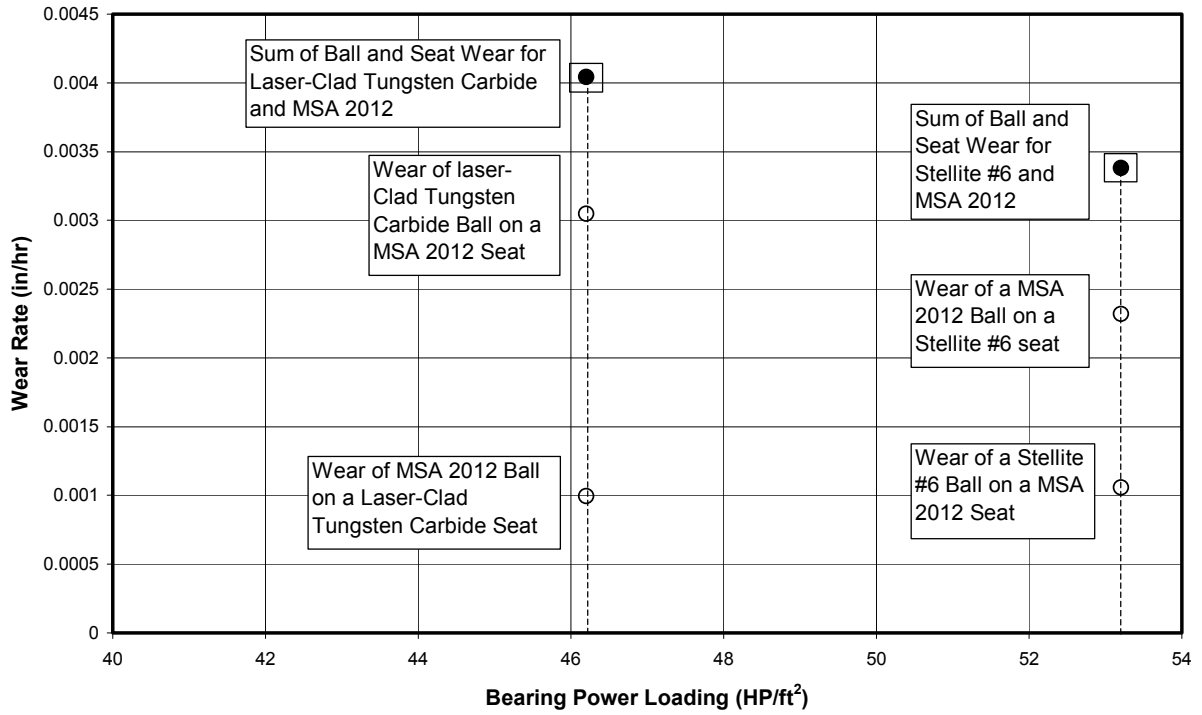
Figure 6.18: Material Combinations Wear Rate as a Function of Bearing Power Loading = $P_C * V_C$

Chapter 7 - Conclusion

The apparent longest lasting zinc pot bearing material seat specimen tested was the laser-clad tungsten carbide on stainless steel. This material showed little wear when tested against other bearing materials. From collected data the wear rate of bearing materials appears linear with time and with contact velocity. This relationship appears to hold for a variety of bearing materials. However, the wear rate as a function of contact pressure appears to be non-linear. The degree of non-linearity is dependent on the bearing material combination.

The data collected by the WVU zinc pot bearing materials tester shows that the machine operates as designed and able to cover the operational range of typical steel mill galvanizing lines. The zinc pot bearing materials tester has numerous safety features built into it that make it safe to operate.

In a paper titled "Dynamics of Journal Bearings on the Stabilizer and Sink Rolls in a Zinc Pot" written by Mark Bright and Gregory Becherer of the Metaullics Systems Company the lubrication of zinc pot bearings was addressed. The type of lubrication regime in zinc pot bearings depends on lubricant viscosity (Z), bearing rotational speed (N) and bearing load pressure (P). These three variables determine whether the bearings are operating in one of three regimes: boundary lubrication, mixed film lubrication or hydrodynamic lubrication. Hydrodynamic lubrication produces a complete separation of the two bearing surfaces, where in boundary lubrication there is virtually no fluid-film present. In order to determine which regime that the bearings are operating in, the friction coefficient is plotted as a function of ZN/P. This is commonly known as a Striebeck Curve. In this paper a sheet speed of 600 ft/min, a sheet tension of 6000 lb_f and

a zinc viscosity of 3.3 centipoise determined a ZN/P value of 0.984. This value indicates that the bearings are operating in the boundary lubrication regime.

References

[1] K. Chang, G. Psaros, J.J. Brinsky, R.L. Nester, R. Carter, V. Sikka, "New Material Research and Life Improvement for Pot Hardware in Continuous Hot-Dipping Processes," Steel Industry of the Future.

[2] R.E. Bond, J.L. Loth, R.W. Guiler, and N.N. Clark, "Lubricity Problems and Solutions for a Methanol Fueled Gas Turbine," Rheology and Fluid Mechanics of Nonlinear Materials, FED-Vol 252.

[3] American Society for Testing and Materials, Standard Handbook Method for Measurement of Lubricity of Aviation Fuels by Ball on Cylinder Lubricity Evaluator, D5001-90a(1995)a American Society for Testing and Materials, West Conshohocken, PA., 1999.

[4] Lubrizol Corporation, Lubrizol Scuffing BOCLE, http://www.lubrizol.com/referencelibrary/news, Lubrizol Corporation, 2000.

[5] Rabinowicz, Ernest, Friction and Wear of Materials, John Wiley & Sons, Inc., New York, 1995, pgs 239-250.

[6] Teck Cominco LTD, "Continuous Galvanizing Line (CGL) Submerged Hardware Research," October 1996.

[7] Teck Cominco LTD, "Study of Hydrodynamic Bearing Operation with Cominco's Full Journal Bearing Test Rig," November 1999.

[8] Oberg, Eric, and Jones, F.D., Machinery's Handbook, 16th Edition, The Industrial Press, New York, NY, 1962, pg. 509.

[9] H. Zoz, H.U. Benz, K. Huttebraucker, L. Furken, H. Ren, R. Reichardt, "Stellite bearings for liquid Zn-/Al-system with advanced chemical and physical properties by MA," Metall 54, Jahigang, November 2000.

[10] El-Madg, M.A. Shaker, R. Hechor, A.E. Nasser, Mechanical Behavior of Stellite 6 Produced by Powder. Metallurgicaly Process, 6th Int. Conf. On Mechanical Design and Production (mpd-6). Cairo, Egypt. 1996.

[11] B.G. Seong, S.Y. Hwang, M.C. Kim, K.Y. Kim, "Reaction of WC-Co coating with molten zinc in a zinc pot of a continuous galvanizing line," Surface and Coatings Technology, 138 (2001) 101-110.

[12] P. Gilorimini, P. Durighello, F. Nonne, "Bearing tester for bath hardware material," Arcelor Research/IRSID, Galvanizers' Association Meeting, October 2002.

[13] Ware, R.T., "Design and Construction of Zinc Pot Bearing Material Wear Tester," Thesis, West Virginia University, Department of Mechanical and Aerospace Engineering, August, 2002.

Appendix A - Quick Basic® Data Acquisition Computer Program

DIM L AS INTEGER   *'dimensions load output variable as an integer*

DIM Q AS INTEGER   *'dimensions torque output variable as an integer*

DIM TP AS INTEGER   *'dimensions temperature output variable as an integer*

DIM R AS INTEGER   *'dimensions RPM output variable as an integer*

DIM lv AS INTEGER   *'dimensions load input signal as a single precision*
                                   'floating point variable

DIM tqv AS INTEGER   *'dimensions torque input signal as a single precision*
                                   'floating point variable

DIM tpv AS INTEGER   *'dimensions temperature input signal as a single precision*
                                   'floating point variable

DIM rv AS INTEGER   *'dimensions RPM input signal as a single precision*
                                   'floating point variable

DIM sampletime AS LONG   *'dimensions test duration time as an integer variable*

DECLARE FUNCTION adcin% (chan AS INTEGER, datv AS SINGLE)
'declares the subroutine function found at the end of this program and dimensions the
'channel as an integer and dimensions the voltage signal as a single precision floating
'point variable

CLS   *'clears data output screen before data collection begins*

ON TIMER (1) GOSUB pace: *'sets timer at 1 second interval and branches to the*
                                          'subroutine

TIMER ON   *'turns on timer*

FILE = 7090505   *'sets the file name to month/day/time based on user input*

PRINT "File Name=" ; FILE   *'prints the file name to the output screen*

PRINT " TIME   LOAD   TQ   TEMP   RPM   "
'prints titles at the top of each respective column of data on the output screen

OPEN "A:\7090505.txt" FOR OUTPUT AS #1
 'opens drive A to output data to a floppy disk

PRINT #1, "File Name=" ; FILE   *'prints file name defined above to the floppy disk*

PRINT #1, " TIME(mV)   LOAD(mV)   TQ(mV)   TEMP(mV)   RPM(mV) "
'prints titles at the top of each respective column of data to the floppy disk

sampletime = 0   *'sets sample time to 0 at the beginning of the test*

TIMER ON   *'turns timer on*

DO   *'starts the beginning of a loop*

LOOP UNTIL sampletime > 900
'maintains the loop until the sample time is greater than 900 seconds

STOP   *'stops the loop once the sample time has reached 900 seconds*

pace: *'sets the channels that the subroutine will scan*

    L = acdin (5 + 64, lv)   *'load is on channel 5 with a gain of 100*

    TQ = acdin (1 + 64, tqv)   *'torque on channel 1 with a gain of 100*

    TP = acdin (3 + 32, tpv)   *'temperature on channel with a gain of 10*

    R = acdin (2, rv)   *'RPM on channel 2 with a gain of 1*

PRINT USING " ###,###   ####.####   ####.####   ####.####   ####.#### ";
sampletime; lv; tqv; tpv; rv
'prints the output data to the output screen with the user specified number of
'significant figures

sampletime = sampletime + 1   *'iterates sample time by 1 second in the loop*

PRINT #1, sampletime, lv, tqv, tpv, rv
'prints the time and collected data to the floppy disk

RETURN   *'returns subroutine to the loop*

'beginning of subroutine

FUNCTION adcin% (chan AS INTEGER, datv AS SINGLE)
'begins function rpocedure and dimensions channels as integers and data voltage signals
'as floating point variables

    CONST adr = &H300   *'sets the base address of the RTI 800 board at 300H*
    DIM dat AS INTEGER   *'dimensions data signal as integer*

```basic
'
'set channel
'
OUT adr + 1,  chan      'goes out to RTI 800 board to the multiplexer/gain select
'                       'byte at abse address 300H + 1 where the channel signal
'                       'gain is set
'start conversion
'
OUT adr + 2,  0         'goes out to the RTI 800 board to the convert command byte
'                       'at base address 300H + 2 which is not used
'
'wait for end of conversion
'
DO      'starts the beginning of a loop

LOOP UNTIL (INP (adr)  AND  &H40) > 0
'executes a relational test to check for the data signal

dat = INP (adr + 3) + (INP (adr + 4)  AND  &HF) * 256
'collects 8 bits of data signal at base address 300H + 3 and collects 4 bits of data
'at base address 300H + 4 which is added to the first 8 bits to create a 12 bit
'signal

IF  (dat  AND  &H800) >  0 THEN
            dat = dat OR &HF000
'checks if data signal is greater that 0, if it is true then the program writes the
'data to the output screen, if it is false then the program writes a row of zeroes
'to the output screen

END IF      'ends IF statement

datv = dat * 20000!  /  4095!
'converts the collected 12 bit binary signal to a voltage signal

adcin = dat     'sets subroutine equal to the data signal

END FUNCTION       'ends subroutine function
```

Appendix B - Calibration Procedure

The torque strain gage beam was calibrated by attaching a string to the beam and hanging know weights form the string. The string was attached to a pulley, which transfers the force to the horizontal direction. The output voltage was read for each respective weight and a calibration curve was then constructed. The same curve is obtained for increasing or decreasing loads. The calibration curve for the torque strain gage beam can be seen in Figure B.1.
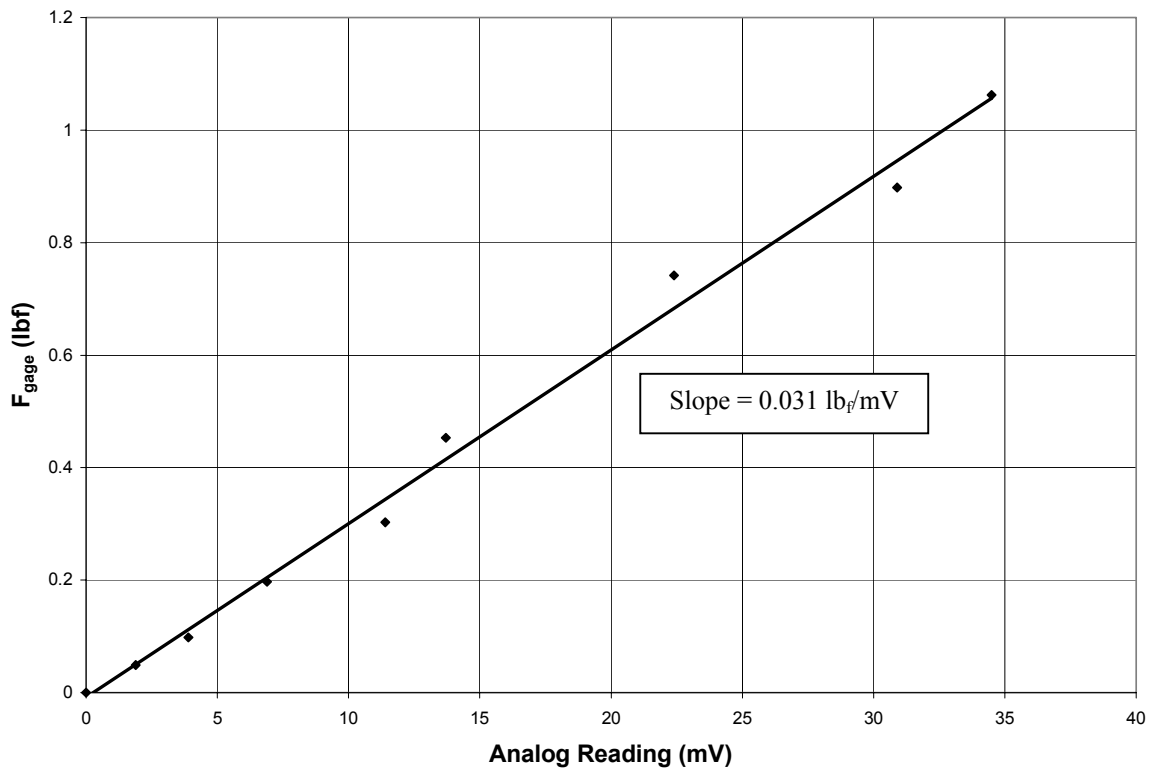
Figure B.1: Calibration Curve for Torque Strain Gage Beam F$_{Gage}$ with Moment Arm l$_{Gage}$=6.75-inch

The load cells were calibrated in a similar fashion by placing known weights on the cup torque transfer plate and recording the output voltage. It was then possible to generate a calibration curve for the load cells as seen in Figure B.2.
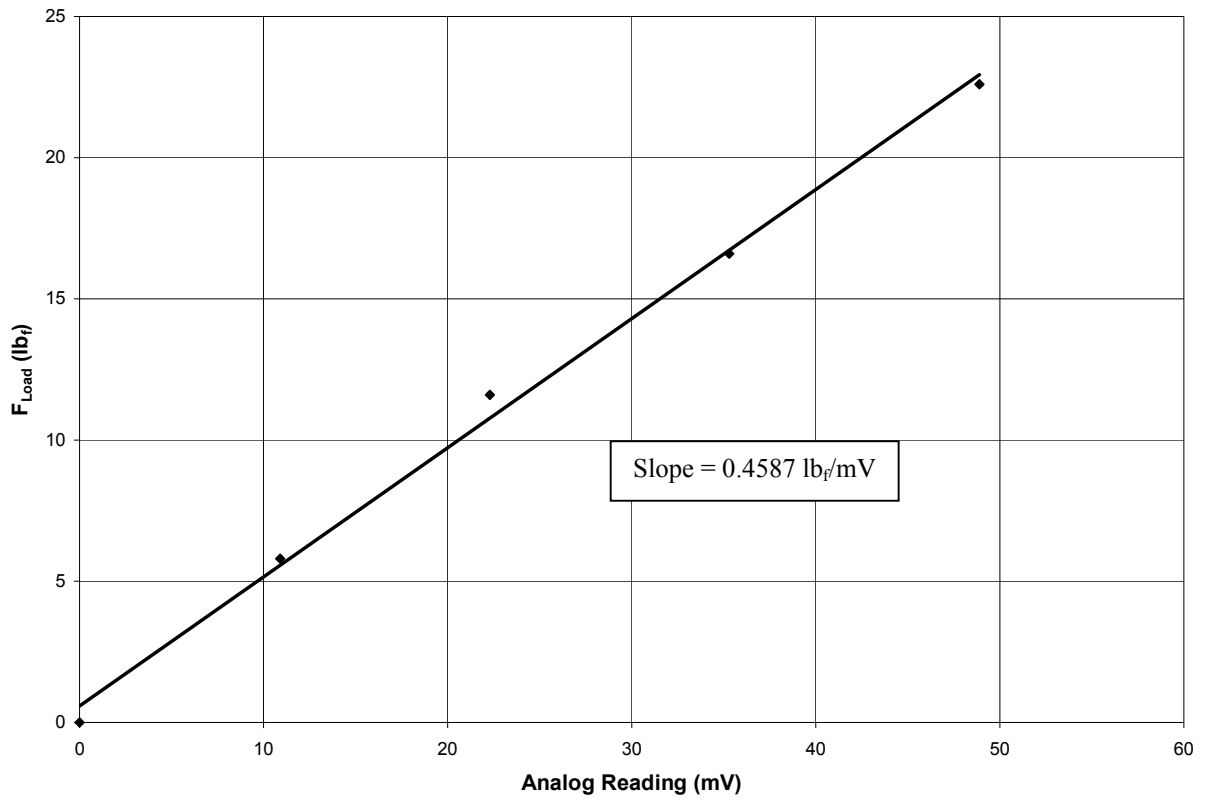
Figure B.2: Calibration Curve for Load Cells

The RPM sensor was calibrated by attaching the sensor to a vertical mill and reading the voltage output from the RPM meter at various speeds. A calibration curve for this instrument can be found in Figure B.3.

Figure B.3: Calibration Curve for RPM Sensor

A calibration of the type K thermocouple was not necessary, because the manufacturer provided a calibration constant. The constant provided was 1˚F / mV for the type K thermocouple and thermometer readout.

Appendix C - Zinc Composition

Table C.1: Chemical Composition Analysis for Molten Zinc Used in Testing.

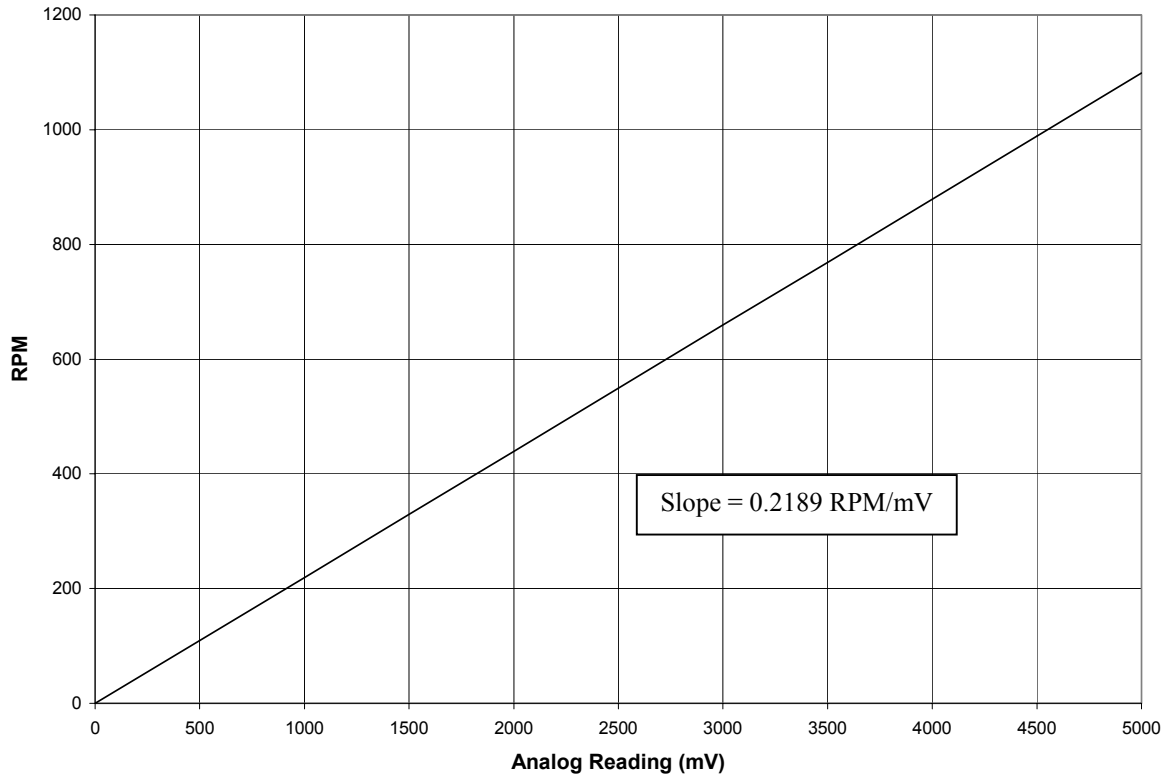|	Al %	Cu %	Fe %	Pb %	Cd %	Si %	Zn %
Zinc Start-up Material							
Bulk Material	0.1593	0.0005	0.0131	0.0019	0.0010	<0.0003	99.82
Static Test							
Alloy 4 500h	0.1688	0.0005	0.0156	0.0022	0.0010	<0.0003	99.81
Alloy 4-1 500h	0.1689	0.0004	0.0163	0.0021	0.0008	<0.0003	99.81
Alloy 4-2 500h	0.1674	0.0004	0.0147	0.0020	0.0007	<0.0003	99.81
Alloy 4-4 500h	0.1723	0.0005	0.0167	0.0022	0.0010	<0.0003	99.81
Dynamic Test							
Top Dross 48h	0.4400	0.0004	0.0169	0.0019	0.0009	<0.0003	99.54

Average (n=3)

Appendix D - Error Analysis

An error analysis was performed on the friction coefficient and wear rate data collected. In order to determine the uncertainty of the friction coefficient, $\omega_{\mu F}$, the following formula was used.

$$\omega_{\mu_F} = \left[\left[\left(\frac{\partial \mu_F}{\partial F_{gage}} \right) * \omega_{F_{gage}} \right]^2 + \left[\left(\frac{\partial \mu_F}{\partial F_{load}} \right) * \omega_{F_{load}} \right]^2 \right]^{1/2} \qquad \textbf{(D.1)}$$

By taking the required partial derivatives of Equation 5.1 and using them in the above equation, the following relation results.

$$\omega_{\mu_F} = \left[\left[\left(\frac{13.5}{F_{load}} \right) * \omega_{F_{gage}} \right]^2 + \left[\left(\frac{-13.5 * F_{gage}}{(F_{load})^2} \right) * \omega_{F_{load}} \right]^2 \right]^{1/2} \qquad \textbf{(D.2)}$$

Next, the uncertainties of the load, ω_{Fload}, and torque, ω_{Fgage}, were determined. This was done by assuming the uncertainty for each variable to be three times the standard deviation of the load cells and torque strain gage beam. In order to determine each respective uncertainty, a known weight was applied to the load cells and torque strain gage beam in the same manner as was done for their calibration, as seen in Appendix B. The known weight was applied twenty times and the reported output from the load cells and torque strain gage beam was recorded and a standard deviation of this data was determined. The standard deviation of the load cells and torque strain gage beam was found to be 0.0284 lb_f and 0.0195 lb_f respectively. When the standard deviations were multiplied by three and substituted into Equation D.2, the uncertainty of the friction

coefficient can be determined from Equation D.3 and shown by error bars on the applicable data Figures.

$$\omega_{\mu_F} = \left[\left[\left(\frac{13.5}{F_{load}} \right) * (0.0585) \right]^2 + \left[\left(\frac{-13.5 * F_{gage}}{(F_{load})^2} \right) * (0.0852) \right]^2 \right]^{1/2} \qquad \textbf{(D.3)}$$

The uncertainty of the wear rate, ω_{wr}, was determined in a similar manner to that of the friction coefficient. The uncertainty of the wear rate was defined as the following.

$$\omega_{wr} = \left[\left[\left(\frac{\partial (wr)}{\partial (wear\,depth)} \right) * \omega_{wear} \right]^2 + \left[\left(\frac{\partial (wr)}{\partial t} \right) * \omega_t \right]^2 \right]^{1/2} \qquad \textbf{(D.4)}$$

By taking the partial derivatives of the relationship for wear rate, Equation 5.5, the following uncertainty for wear rate is found.

$$\omega_{wr} = \left[\left[\left(\frac{1}{t} \right) * \omega_{wear\,depth} \right]^2 + \left[\left(\frac{-wear\,depth}{t^2} \right) * \omega_t \right]^2 \right]^{1/2} \qquad \textbf{(D.5)}$$

The uncertainty in the wear depth, $\omega_{wear\,depth}$, was taken as half of the smallest scale division on the optical magnifier divided by $\sqrt{2}$, which is equal to 0.0014-inches. The uncertainty in the time measurement, ω_t, was determined to be 1 minute based on clock used for time keeping. With the use of these uncertainties, a relation for the uncertainty in the wear rate was determined.

$$\omega_{wr} = \left[\left[\left(\frac{1}{t} \right) * (0.0014) \right]^2 + \left[\left(\frac{-wear\,depth}{t^2} \right) * \left(\frac{1}{60} \right) \right]^2 \right]^{1/2} \qquad \textbf{(D.6)}$$

The final uncertainty to be determined was the contact pressure, P_c. The contact pressure is found by dividing the load by the horizontal projected area, A_h. The uncertainty of the contact pressure, ω_{Pc}, is defined as follows.

$$\omega_{P_C} = \left[\left[\left(\frac{\partial P_C}{\partial A_h} \right) * \omega_{A_h} \right]^2 + \left[\left(\frac{\partial P_C}{\partial F_{load}} \right) * \omega_{F_{load}} \right]^2 \right]^{1/2} \qquad \textbf{(D.7)}$$

By substituting the required partial derivatives of the contact pressure into the above equation, an uncertainty for the contact pressure was determined.

$$\omega_{wr} = \left[\left[\left(\frac{-F_{load}}{A_h^2} \right) * \omega_{A_h} \right]^2 + \left[\left(\frac{1}{A_h} \right) * \omega_{F_{load}} \right]^2 \right]^{1/2} \qquad \textbf{(D.8)}$$

The uncertainty for the load cells is the same as determined previously, 0.0852 lb$_f$. The uncertainty of the horizontal projected area was taken as half of the smallest scale division on the optical magnifier squared and multiplied by π, which is equal to 0.000013-inches. With the use of these two uncertainties the following equation for the uncertainty of the contact pressure was determined.

$$\omega_{wr} = \left[\left[\left(\frac{-F_{load}}{A_h^2} \right) * (0.000013) \right]^2 + \left[\left(\frac{1}{A_h} \right) * (0.0852) \right]^2 \right]^{1/2} \qquad \textbf{(D.9)}$$

The above Equations, D.3, D.6 and D.9, were used to determine the error in the friction coefficient, wear rate and contact pressure.